UPTEC W 23027
Examensarbete 30 hp
Juni 2023

UPPSALA UNIVERSITET

SLU

Soil compaction and the effect on infiltration in urban green environments

A study based on field measurements and HYDRUS 1D modelling

Anastasia Novikova

Civilingenjörsprogrammet i miljö- och vattenteknik

UPPSALA UNIVERSITET

SLU

Soil compaction and the effect on infiltration in urban environments

Anastasia Novikova

Abstract

The consequences of recent flooding and extreme rain events have highlighted the importance of proper urban planning and preventative measures for storm water management. As cities become more urbanized the significance of permeable surfaces such as parks and other urban green spaces increases which infiltrate the water into the ground. Agricultural research has for many years emphasized the effect of compaction on soil parameters and how, not only the crop yield reduces but also how the infiltration decreases. This thesis aims to study how the infiltration rate, bulk density and soil resistance changes with compaction through field experiments where a vehicle is let to roll over an urban green area. The thesis will also simulate rainfall over five theoretical soils that can be found in urban environments exposed to compaction to determine what significance compaction has on surface runoff. The modelling software HYDRUS-1D will be used so simulate rain fall events on the different soils. The rain events simulated will be based on the five hyetographs that best represent Sweden's rain events, based on historical data. A CDS rain will be simulated as well. They will be simulated for a 2, 10 and 100 year return period. A literature study will also be conducted to determine how relevant freeze-thaw cycles are to the soil parameters.

It is since previously known that freeze-thaw cycles can improve aggregate stability, increase soil particle fragmentation which can lead to less soil penetration resistance and even partially return the soil conditions to those prior to compaction, but the process does not extend to layers beyond 40 cm. The field experiment results showed a clear decrease in infiltration rate with increasing number of vehicle passes. There was no clear correlation between bulk density and the number of vehicle passes. This result is attributed to the relatively light weight of the vehicle used as well as the heterogeneity of the soil. The cone penetration measurements showed an increasing resistance with increasing number of vehicle passes for only one of the three measured sites, with the most resistance being measured in a pathway on the green area. The insignificant results of one of the two other sites are attributed to wet weather conditions and unknown underlying material. The HYDRUS 1D simulations showed that a higher sand content mitigates the effects of soil compaction and leads to less runoff. The soil classified as sand (93% sand) had no runoff, the loamy sand (80% sand) had mild runoff. When comparing a sandy loam (60% sand) and a clay soil it is concluded that the sandy loam is more sensitive to soil compaction as more compaction leads to more runoff compared to the non-compacted scenario. The clay soil has little variation between the compaction scenarios but has generally more surface runoff in total. Soil texture therefor affects the surface runoff more than soil compaction. Most amount of runoff was generated by the two hyetographs which had a late peak intensity, most likely due to the soil already being saturated when the peak occurs. The runoff also increases with the return period of the rain event for both the hyetographs and the CDS rain.

Teknisk-naturvetenskapliga fakulteten

Uppsala universitet, Utgivningsort Uppsala/Visby

Handledare: Johan Kjellin Ämnesgranskare: Mats Larsbo

Examinator: Antonio Segalini

UPPSALA UNIVERSITET

SLU

Soil compaction and the effect on infiltration in urban environments

Anastasia Novikova

Sammanfattning

De extrema skyfall och deras medföljande konsekvenser i Sverige har betonat behovet av en adekvat stadsplanering och dagvattenhanteringssystem. Ju mer urbanisering expanderar desto mer ökar vikten av de gröna ytornas förmåga att kunna infiltrera det inkommande vattnet. Forskning inom jordbrukssektorn har länge understrukit relevansen av kompaktering i jorden och vilka konsekvenser detta kan ha för infiltration, skörden etc. Existerande skyfallsmodelleringar tar sällan hänsyn till kompaktering och hur detta kan påverka avrinningen.

Detta projekt har som syfte att utvärdera hur jordkompaktering kan påverka infiltrationen och därmed även risken för avrinning vid skyfall. I detta arbete kommer de fem hytograferna, som har tagits fram av SMHI baserat på historiska regn, samt ett CDS-regn simuleras över fem olika jordar med tre olika kompakteringsgrader. Modelleringen kommer at utföras med HYDRUS-1D som simulerar skyfall över en jordprofil vars parametrar går att modifiera. Hur kompaktering påverkar jorden kommer även att mätas i fält med mätningar på jordens skrymdensitet, motstånd samt infiltration efter ett fordon har låtits passera över en sträcka på tre urbana grönområden i Uppsala. Hur frysning-tinings cykeln påverkar jorden kommer också att studeras som ett komplement i form av en litteraturstudie.

Resultaten visar att frysning-tining cykler hjälper att fragmentera större jordpartiklar och kan främja stabiliteten i lerhaltiga jordar. Det har också visat att minska på tryckmotståndet i jorden vid mätningar med penetrologger. Fältförsöken visade att infiltrationen minskade tydligt med ökade antal passage med ett fordon. Jordmotståndet ökade med antal passage för endast en av de tre jordarna som testades men mest motstånd kunde identifieras på gångstigar vid två av jordarna som testades, vilket påvisar att en liten kontinuerlig belastning under en längre tid leder också till kompaktion i jorden. Inget samband kunde hittas mellan skrymdensitet och ökade antal passage med fordon, detta förmodligen på grund av den höga heterogeniteten i jorden. Alternativt i kombination med att fordonet var för lätt för att ha en effekt ned till 10-15 cm djup där proverna togs. HYDRUS-simuleringarna visade att en högre sand-halt i jorden leder till mindre avrinning samt att "sandy loam" var den känsligaste jorden för kompaktering. Lerjorden har minst variation mellan de olika kompakterings-scenarion men resulterade oavsett i mest avrinning jämfört med alla andra jordar. Därmed är jordkomposition en större drivande faktor för avrinning än kompaktering. De hytograferna som ledde till mest avrinning var de med en sen maxintensitet, med största sannolikhet då marken redan är mättad när denne inträffar. Avrinningen ökade även med ökad återkomsttid för regnen, både för de fem hytograferna och CDS-regnet.

Teknisk-naturvetenskapliga fakulteten

Uppsala universitet, Utgivningsort Uppsala/Visby

Handledare: Johan Kjellin Ämnesgranskare: Mats Larsbo

Examinator: Antonio Segalini

UPPSALA UNIVERSITET

SLU

Soil compaction and the effect on infiltration in urban environments

Anastasia Novikova

Populärvetenskaplig sammanfattning

På senare år har många städer i Sverige upplevt en många översvämningar, särskilt under sommarmånaderna. Det har lett olika konsekvenser, allt från hindrade passage genom tunnlar till flera översvämmade källare. I och med fler vägar som byggs, parkeringar som anläggs och grönområden som försvinner så minskar den ytan i städer som har förmågan att infiltrera det inkommande regnvattnet i marken. Det innebär en ökad betydelse av de grönområden som finns kvar i städerna. Något som jordbrukssektorn i många år poängterat är konsekvenserna av kompaktering på jorden, då detta har lett till minskad infiltration och skörd. Detta projekt har ämnat att överbrygga klyftan mellan dessa sfärer för att bättre förstå hur kompaktering kan påverka markens egenskap att infiltrera de stora mängderna vatten som kommer vid extrema regn.

Många kommuner utför så kallade skyfallskarteringar, där man utvärderar översvämningsrisken för olika delar av staden vid ett extremregn. Det många skyfallskarteringar missar är delvis de grönytor som finns i städerna men även hur eventuellt kompakterade grönytorna är.

Denna studie har använt sig av fem regnmönster sammansatta av SMHI för att simulera över fem olika jordar, med varierande komposition av lera, silt och sand, samt varierande grad av kompaktering. Dessa simuleringar kommer att modelleras i ett program. I samband med detta kommer det även utföras fältförsök där en bil passerar över en yta flera gånger på tre olika jordar, där man sedan mäter skrymdensiteten, infiltrationen och tryckmotståndet på jorden. Detta för att utvärdera hur jordens egenskaper förändras med kompaktering. Eftersom att vi bor i ett kallt klimat, så genomgår jorden kontinuerliga cyklar av frysning-tining varje vinter. Även denna process har en effekt på jordens egenskaper som också ska utredas i denna studie.

Utvärdering av frysning-tining processen visade att för sand-haltiga jordar så hjälper denna process till med fragmentering, medan för ler-haltiga jordar ökade stabiliteten i jorden. Vid mätningar där jordens tryckmotstånd mäts såg man att tryckmotståndet minskade efter frysning-tinings processen. Fältförsöken med fordonet visade inte att skrymdensiteten ökade med ökade antal körningar med fordonet på samma yta, med största sannolikhet på grund av att fordonet var för lätt för att ha en effekt så långt ned i marken (10 - 15 cm djup). Marken är även känd att vara högt varierande och det är svårt att ta representativa prover. Motståndsmätningarna visade att motståndet ökade med antalet passage för endast en av de tre jordarna som testades. Infiltrationsmätningarna visade en tydlig minskning med ökade antal passage med bil på alla tre jordar som testades. Datasimuleringarna över de fem jordarna visade att avrinning ökar med ökad kompaktering. Jorden i kategorin "sandy loam" var mest känslig för kompaktering men att mest avrinning totalt sker från lerjordar, oavsett hur kompakterad den blir. Dessutom får man mindre avrinning ju med sand jorden innehåller. Därmed går det att se ett större samband mellan avrinning och komposition på jorden, snarare än avrinning och kompaktering.

Teknisk-naturvetenskapliga fakulteten

Uppsala universitet, Utgivningsort Uppsala/Visby

Handledare: Johan Kjellin Ämnesgranskare: Mats Larsbo

Examinator: Antonio Segalini

Preface

This project is done as a master thesis for the Master Programme in Environmental and Water Engineering. I want to thank my supervisor Johan Kjellin from Tyréns and subject reviewer Mats Larsbo from the Swedish University of Agricultural Sciences for your guidance and expertise throughout this thesis. A special thank you to Sara Ekeroth at Tyréns for your guidance, field assistance, programming help and valuable feedback.

Thank you to my classmate Felix Jansson for helping me with my field work when no one else could, despite the rainy weather. Thank you to my dorm mate Fredrik Plane for helping me learn coding in Python during late evenings.

A last thank you to my friends and family for your love and support. I am proud of both myself and my classmates for the the hard work we've put in these five years, but most of all I'm grateful for the wonderful memories we've created in Uppsala together. Thank you.

Abbreviations

AMA Allmän material och arbetsbeskrivning - General material and work description

CDS Chicago Design Storm

FTC Freeze-thaw cycle

GUI General User Interface

SLU Sveriges lantbruksuniversitet - Swedish University of Agricultural Sciences

SMHI Sveriges meteorologiska och hydrologiska institut - Swedish Meteorological and Hydrological Institute

Contents

1 Introduction

For the past decades, an increase in intense rainfall can be observed in multiple places around the world. Globally, around 6 000 lives were claimed in 2020 as a result of flooding, with more than 34 million affected by the events, left injured or homeless (Statista n.d.). During the last 30 years, rainfall has increased in Sweden with extreme rainfall with higher volume and intensity than a ”10 year rainfall event” occurring on multiple locations every year (MSB 2013). On top of this, the risk of flooding significantly increases due to expanding urbanization (Simonovic & Nirupama 2007). As urbanization expands, the natural infiltration reduces significantly due to reduced exposed soils, increase in compacted soils on construction sites, installment of walkways, roads, etc. (Pitt et al. 2008). The significance of permeable surfaces like green areas and parks become essential to infiltrate the incoming rainfall and the soils capacity to infiltrate the incoming water plays a large role in the risk of flooding. Soil type, soil saturation and soil compaction are a few examples of the soils dynamics that can affect the rate of infiltration.

Previous research has highlighted the importance compaction has on infiltration rate (Pitt et al. 2008), and how an increasing compaction leads to a decrease in infiltration. This in turn increases the risk of surface runoff and eventually flooding (Gregory et al. 2006). During urbanization, extensive and involuntary soil compaction still occurs unintetinally during landscaping projects, due to the use of heavy machinery (Batey & McKenzie 2006). This results in a change of the soil characteristics, potentially significantly decreasing the soils ability to infiltrate rainfall.

Intense rainfall events are hard to predict and often very local, making any short term solutions hard to adapt and in the end inadequate, which increases the significance of long term and preventive urban planning (MSB 2013). One way to map out the areas more vulnerable to flooding is using cloudburst simulation models. Although soil properties are included in common cloudburst modelling software like MIKE+ and HEC-RAS, which simulate runoff from soil profiles in 2D/3D, Pitt et al. (2002) highlighted that storm water runoff based on models that do not include compaction can provide consequential errors in soil infiltration simulations. Therefore, further understanding and inclusion of soil compaction in runoff models and the succeeding effect on soil properties is needed. This report will explore the risk of runoff with different soil's varying bulk densities using HYDRUS-1D, which is a modeling software for analysis of water transport through a soil profile. The software also has the ability to adapt to different soil types, taking into consideration varying bulk densities as well as hydraulic parameters which are known to change with compaction. Soil compaction has long been an issue within the agricultural sector and the succeeding effects it has on crop yield. Therefore, a substantial amount of information on the topic is sourced from the agricultural sector and this report also aims to adapt that knowledge to the urban landscaping sector.

Commonly used is Swedish runoff modelling is Chicago Design Storms (CDS-rain) (Svenskt Vatten 2011) which simulates a rainfall event with a clear peak. Simultaneously, Olsson et al. (2017) has recently developed empirical hyetographs based on historical rain data collected throughout Sweden. Creating a more accurate estimation of surface runoff with both CDS rain and hyetographs, as well as taking into consideration the varying soil properties with compaction can contribute to better urban planning, storm water management and flood control which can help mitigate flood consequences.

1.1 Aim

The aim of this project is to explore the varying soil characteristics during compaction, as well as the impact these factors have on soil infiltration and potential runoff. Based on existing theory surrounding soil characteristics, five soils will be modeled based on soil parameters collected from literature. Additionally, compaction will be simulated in the field followed by sampling to evaluate the direct effect of compaction. The dual method approach aspires to validate the results and also highlight insecurities associated with both methods. The work aims to bridge the gap between agriculturally bound knowledge and city landscape planning regarding soil compaction and general management.

1.2 Problem statement

- What are some sources to soil compaction in urban environments?
- How does the freeze-thaw process affect soil properties?
- How does the infiltration rate vary with soil compaction?
- How does the soil properties vary with soil compaction?
- How does soil compaction affect the surface runoff in urban environments?
- What significance does soil compaction have on soil infiltration rate compared to other parameters?

2 Theory

2.1 Soil dynamics

Soils are made up of three components; water, air and solids. The latter consisting of different sized particles e.g clay, silt, sand, gravel etc. The pores between the solid particles is either filled with air or with water. Soil texture, also known as soil particle distribution, can be classified using a particle size distribution classification chart as seen in figure 1 and determines some of the soils characteristics based on the composition (Rai et al. 2017). Note that the chart does not take into account the soils organic matter content.

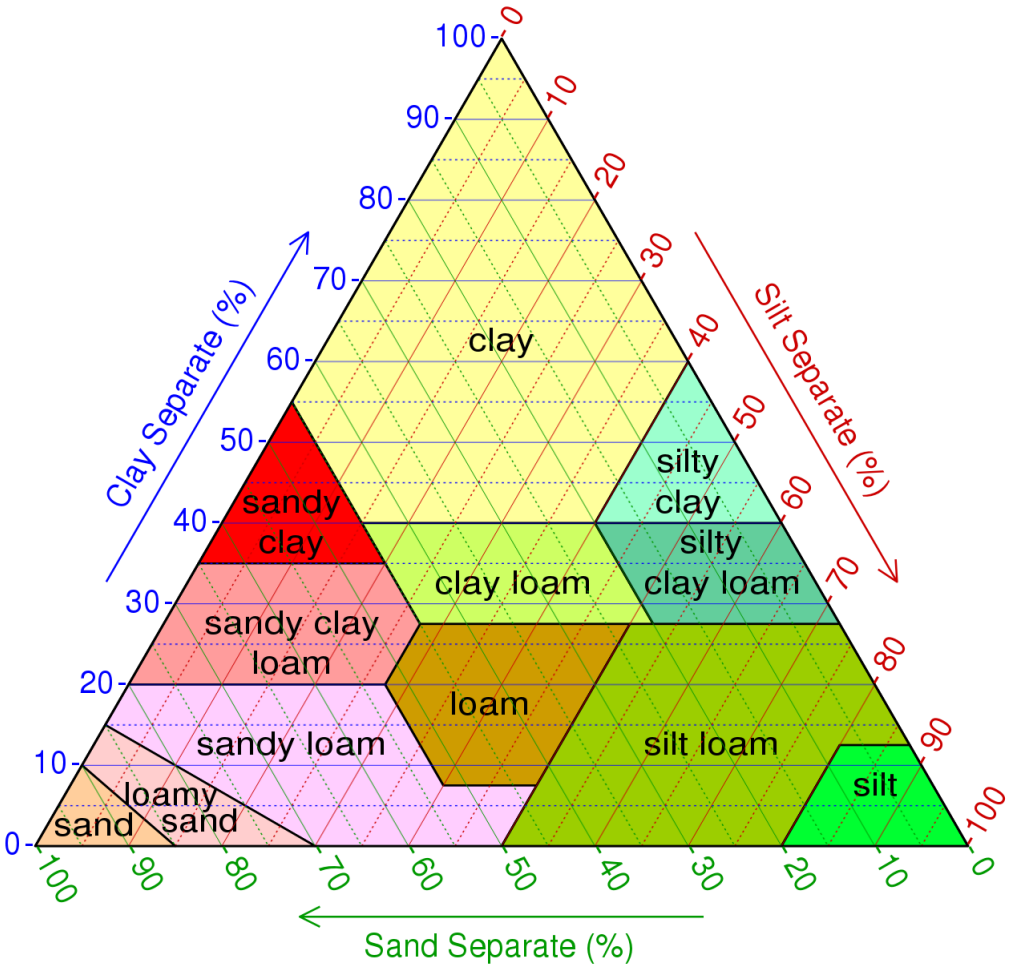

Figure 1: The United States Department of Agriculture particle size distribution classifications (Wikipedia).

The soils porosity is a measure of the percentage of air and water filled pores in the soil. The porosity of sandy soils can range from 30 - 40%, 40- 45 % in loam soils and 45 - 55% in clay (Rai et al. 2017).

A soils dry bulk density is referring to the mass soil in relation to the total volume, including the air filled pockets. The dry bulk density changes if the sample is compacted or ruffled up, as the pore system is part of the total volume unit (Eriksson et al. 2019). Bulk density can give a rough

estimation of what the compactness, infiltration rate, texture and water storage capacity of the soil is. Typical bulk densities range from 1.0 - 1.1 g/cm^3 for sand, 1.1 - 1.3 g/cm^3 for silt and 1.3 - 1.6 g/cm^3 for clay (Rai et al. 2017).

2.2 Soil compaction

There is no one way to measure soil compaction, but a change in bulk density, soil strength or cone penetrations measurements can be signs of an increase of compaction in the soil (Sharifi et al. 2007). The main reasons for compaction is due to applied force, usually as a result of the use of mechanical aids like tractors, trailers etc. (Batey 2009). Extensive compaction can be observed on e.g. quarry cites (Sinnett et al. 2006) and during remodelling of landscapes (Batey & McKenzie 2006), as heavy machinery is invariably used. Since heavy machinery is the new norm within the agricultural sector, soil compaction and the even deeper subsoil compaction is a common phenomenon seen on farms (Håkansson & Petelkau 1994). Apart from the application of weight, soil compaction has also been observed due to the wheel-slip of vehicles (Davies et al. 1973). Some level of wheel-slip is necessary to achieve traction, but the ultimate amount of wheel-slip is determined by the ballast and load draught of the vehicle. It is indicated that excessive wheel-slip has a higher risk of causing damage to the underlying soil compared to heavier wheel loading for tractors. This effect is more evident the heavier the vehicle is (Davies et al. 1973). For how long the compaction occurs is also a relevant factor, as a longer exposure to compaction can result in a higher resulting bulk density (Gregory et al. 2006). The number of times a vehicle passes a soil can also be detrimental to the level of compaction. A lighter vehicle passing the same soil surface multiple times has been shown to cause more compaction than a vehicle triple the weight passing once (Pulido-Moncada et al. 2019). Apart from vehicles, other sources to compaction include livestock, as they have also been shown to increase the bulk density, degrade soil structure and decrease infiltration rate on pastures (Mulholland & Fullen 1991, Daniel et al. 2002). Even the water droplets from an intense rainfall have been found to decrease the infiltration rate with increasing kinetic energy of the water droplet (Thompson & James 1985).

Regardless of the source, the effect of compaction is heterogeneous throughout the soil. And different measuring techniques and conditions can highlight the effects of compaction in different layers. Studies point towards the effect of compaction being mostly prevalent and persistent in the lower layers, below the depth of 30 cm, according to Håkansson & Petelkau (1994). This has also been noted by Gregory et al. (2006) as during compaction tests, the greatest signs of compaction was noted between 20 -30 cm when measuring soil penetration resistance. A change in bulk density was also noted after the use of heavy machinery in the upper 10 cm and found significant increase in bulk density and decrease in infiltration rate. The resulting compaction and the ability to withstand deformation inevitably depends on multiple factors. The soil type, shear strength, and density determines the bearing capacity of the soil, which is one of the factors (Batey 2009). Apart from the soils individual characteristics, the force applied at the time of compaction as well as the moisture content can be determining features (Batey 2009). When applying the same pressure to a wet soil (24 - 25% moisture content) and a dry soil (11 - 13% moisture content), the bulk density and total porosity significantly changes only in the wet soil (D'Acqui et al. 2020). The soil moisture profile also affects how deep the applied force

is channeled through the soil. Force applied on a dry top layer sitting on a wet layer could be transmitted further down, compressing the more sensitive wet layer underneath. In the reversed scenario, with a dry bottom soil and a wet top soil, only the top soil would experience significant compression. In the case of a completely dry soil, an applied force would not cause a significant amount of compaction as previously mentioned (Batey 2009).

Another noteworthy factor is the amount of organic matter content in the soil. Although dependant on the moisture content at the time of applied force, a higher organic matter content can help reduce the effects of compaction (Ekwue & Stone 1995). The reduction of compaction with increasing organic matter content is thought to have a higher effect at a higher moisture rather than at a low moisture content (Soane 1990). This is most likely due to the increase of the compacted soils water retention capacity, as well as enhancing the saturated hydraulic conductivity (Ohu et al. 1985).

It is also important to highlight that compaction is not permanent, the soil has an ability to restore itself. Goutal et al. (2012) found that a lesser compacted soil showed no traces of compaction in the upper layer (0 - 10 cm) after the monitoring period of 3 years and the lower layer (10 - 20 cm) had significantly decreased during the same period. The more compacted site only showed less compaction in the upper layer (0 - 10 cm). The recovery was attributed to the shrink-swell process of clays due to fluctuation in moisture content.

2.3 Infiltration rate and hydraulic conductivity

Infiltration is the process of which water penetrates the ground surface, entering the soil. Infiltration is highly dependant on the texture and structure of the soil surface, but also whether or not the soil profile has layers that could restrict the downward movement of the water. The depth of the topsoil and subsoil combined, also affects the rate of drainage (Rai et al. 2017). Once the water has passed the soil-atmosphere barrier, the movement of water is then referred to as percolation. The rate of percolation is dependant on the hydraulic conductivity of the soil material. If the soil profile has two connecting layers with varying pore size the percolation could be hindered. If the water reaches a layer with finer pores, the percolation is slowed down. This would in turn mean a higher build-up of water at the surface as the percolation is slowed down, as well as reducing the depth at which water can be taken up (Weil & Brady 1999). In heavy rainfall events, gravity plays a major role in replenishing the groundwater reserve by removing excess water from the upper layers of soil (Weil & Brady 1999). If the infiltration rate of a soil is lower than a design storm infiltration capacity then the risk of surface runoff greatly increases (Gregory et al. 2006).

It is important to note that hydraulic conductivity does not uphold a consistent value throughout the soil profile, horizontally or vertically. A high level of variability can be identified in experiments conducted in the field, compared to in the laboratory. The field investigators choices regarding method, quality of instruments, assumptions etc. highly influence the results. As well as the chance of including significant macro-pores in the sampled area (Deb & Shukla 2012).

2.4 Soil water retention

The ability to hold water in the soil varies with soil type. Aggregated soil has a typically higher water retention than non-aggregated. Furthermore, Yasuda et al. (2023) found that the size of the particles composing the aggregates are also significant. When the aggregate size is fixed, larger aggregate components lead to a decrease in water retention (WR). Aggregated clay-rich soils can retain water in both the macro-pores, between the soil grains, and in the micro-pores, inside the aggregate structure. Between the grains, water is being held using capillary force, that decreases with increasing soil particle size. With larger particles, the main driving force becomes gravity, pulling the water downwards in the soil profile (Yasuda et al. 2023). Water retention curves (WRC) are used to describe the correlation between the soil water potential and the water content in the soil. Varying bulk densities, which can occur due to compaction, is known to cause changes to the WRC (Tian et al. 2018).

Field capacity, saturation capacity and permanent wilting point are the different water constants used to describe a soils relation to water content. Field capacity is the water content that remains in the soil after drainage, usually occurring 2-3 days after a rain event when the micro-pores are water filled and the macro-pores are filled with both air and water. This can also be described as the water content maintained in the soil at a pressure of -0,33 bar.

The permanent wilting point refers to a state where no water is accessible to plants, which usually occurs around 1 500 kPa as this is the tension required of the plant to extract water from the soil. The permanent wilting point occurs at around 26 - 32% water content for fine-textured soils and 10 - 15% for coarse textured soils.

A fully saturated soil only has water in the pores. Air in the soil is necessary for plants and the absence of it shortens the lifespan of the plant to 2-5 days. Saturation is usually not a long lasting condition and drainage occurs after some time, replacing the water filled pores with air. Drainage in sand rich soils takes a couple hours and 2-3 days in clay rich soils (Rai et al. 2017). Surface runoff evidently occurs when the soil is fully saturated and the hydraulic conductivity is reduced to a minimum.

2.5 Vegetation cover

Different factors affect the infiltration rate into the soil, amongst them is vegetation cover. The plant cover increases the infiltration rate with varying degrees depending on the type of crop (Folorunso et al. 1992). By creating cracks through out the root network (United States Department of Agriculture n.d.*b*), it also reduces the risk of compaction, which is known to decrease infiltration rate. As vegetation cover decreases, the soil becomes more vulnerable to direct force from rain droplets that break apart soil particles which in turn can clog surface pores (*Agronomic Crops Network* n.d.), creating a higher chance of surface runoff (Molina et al. 2007). Simultaneously, compaction is a process that can limit the root growth and has been known to decrease crop yields withing the agricultural sector (Singh & Kaul 2015). An ideal soil for a plant is one that has large air pores but also access to water. A lower porosity, which occurs through compaction, could lead to negative consequences for the plant roots as they encounter larger mechanical resistance in the soil, as well as less access to air (Eriksson et al. 2019).

2.6 Freeze/thaw process

During the winter months in the northern hemisphere, when temperatures drop below 0 degrees Celsius, the soil freezes. An antecedent moisture in the ground leads to the formation of ice from the present water. This process, also referred to as frost heaving, leads to an approximate 10% increase in volume, giving a considerable mechanical effect to the soil structure. This is an important process for clay rich soils, due to the water freezing more slowly, as the ice separates soil clods and improves the soil structure. A slower freezing process gives time for the water to move to the centre of the freezing front with growing ice crystals. The material between the ice crystals will dry out and remain non frozen, creating a heterogeneous freezing profile. For sand rich soils freeze/thaw process has minimal effect on the structure. Coarse soils can have a high moisture content but they have a low amount of small soil particles and Therefore freeze homogeneously throughout the soil profile (Eriksson et al. 2019). Any cracks created in the soil profile due to a freeze-thaw cycle in a coarse grained soil will usually close when the ice melts (Viklander 1997).

In regards to the soil particle itself, a greater amount of fragmentation can be observed in coarser soil particles ($\geq$ silt), as a larger amount of water is bound in an unfrozen state in fine grained soils. Soil particle fragmentation is the formation of cracks in soil particles. Micro-cracks are first generated due to the temperature change in the ground. These later turn into macro-cracks due to the increased pressure of the formation of ice in the soil pores. Water can then seep into the cracks and cause further expansion due to the change in volume when water freezes to ice (Zhang et al. 2016).

Simultaneously, we see that soil aggregates improve and become more stable for clay rich soils after undergoing freeze-thaw cycles. Lehrsch (1998) conducted freeze/thaw experiments on medium to fine grained soils and found that 1-2 freeze-thaw cycles (FTC) are necessary for aggregate stabilization and minimal change occurs thereafter. Different studies have been conducted to determine the effects of the freeze-thaw cycle (FTC) on soil. Chamberlain & Gow (1979) found that for all the four fine-grained soils included in their experiment, all soils experienced a reduction in void ratio and an increase in permeability after the laboratory induced FTCs, emphasizing how the hydraulic properties can change. Further experiments investigated how multiple FTCs affect different textured soils, as studies with only a few FTCs neglect the potential buildup of mechanical stress in the soil. The experiments were conducted on both undisturbed soil and repacked soil, the latter to simulate the loose packing of a ploughed field. The most change in soil structure was noted after 2 -5 FTCs but further cycles were not insignificant. Although the effect decreased after each FTC, there was still an accumulating affect. It is also important to highlight that the initial soil structure and soil texture impacts the significance each FTC has on the resulting soil structure change as the most change was noted in the repacked soil samples. When measuring the infiltration rate after FTCs they either stayed the same or decrease, but this can be attributed to the the lower viscosity of water as it reaches freezing temperature. As well as ice still being present in some soil pores, hindering the flow (Fouli et al. 2013).

It was previously believed that compacted soils undergoing FTCs could regain conditions prior to compaction (Unger & Kaspar 1994), but this was disproved by Voorhees et al. (1978) as the effects of compaction could still be found in the subsoil beneath the tillage depth despite

reoccurring FTCs. FTCs have shown to decrease the penetration resistance of soil with the most affect at the top layer (0 - 10 cm) with decreasing effect further down in the profile down to 20 - 30 cm (Jabro et al. 2014). Håkansson & Petelkau (1994) also pointed out that after a depth of 40 cm the compaction can be regarded as permanent, as periodic FTCs cannot restore the soil at that depth to prior conditions and any mechanical loosening is often difficult and expensive. When comparing FTC with other processes such as shrink-swelling, FTC showed a higher decrease in penetration resistance measurements than the soil not subjected to FTCs (Jabro et al. 2014).

2.7 HYDRUS-1D

HYDRUS-1D is program that simulates water flow through unsaturated/saturated medium, taking into consideration heat transport, solute transport, evapotranspiration and root water uptake if desired. The program solves the Richards equation for water flow. For the root water uptake Feddes reduction function is the most commonly used. HYDRUS is also available as a 2D/3D model, but the 1D version was chosen for this project due to the focus being on the soil profile and its characteristics. The Richards equation is given by:

$$\frac{\partial \theta}{\partial t} = \frac{\partial}{\partial z}[K(\frac{\partial \delta}{\partial z} + 1)] - H \tag{1}$$

θ (%) is the water content in the soil, z is the dimensional coordinate, K is the unsaturated hydraulic conductivity and H is the pressure head (Broekhuizen et al. 2021).

The van Genuchten Mulauem equation describes the water retention and hydraulic conductivity in the soil and has been used in numerous applications since it's publishing in 1980 (Dourado Neto et al. 2011). The equation's application simulates the varying hydraulic conductivity (K(h)) with soil moisture content (θ). The equation is given by:

$$\begin{cases} \theta(h) = \{\theta_r + \dfrac{\theta_s - \theta_r}{[1 + |\alpha h|^n]^m}, \ h < 0 \\ \theta_s, \ h \geq 0 \end{cases} \tag{2}$$

$$K(h) = K_s S_e^l [1 - (1 - S_e^{\frac{1}{m}})^m]^2 \tag{3}$$

Where K_s is the saturated hydraulic conductivity. Furthermore, S_e represents the effective saturation as described by:

$$S_e = \frac{\theta - \theta_r}{\theta_s - \theta_r} \tag{4}$$

$$m = 1 - \frac{1}{n}, n \geq 1 \tag{5}$$

Where h is the water pressure head. θ_r refers to the residual water content and θ_s is the saturated water content. α is the value of air-entry in-versed. The pore size distribution index is given by n and l is related to the pore connectivity. The latter three parameters affect the shape of the soil water retention curve (Wang et al. 2022).

To acquire the parameters described in equation (2) the Rosetta model was used, which is integrated in the HYDRUS-1D GUI. Rosetta is a hierarchical pedotransfer function that converts basic soil data into estimations of the hydraulic parameters fit for van Genuchten Mulaem equation (Schaap et al. 2001).

2.8 Design storm

When evaluating the runoff after a rainfall event the type of rainfall event is relevant to establish the interplay between soil surface and infiltration. Variables such as rainfall intensity (or depth), duration and the frequency of of the event are used to establish a relationship for the hydrological model (Chow et al. 1988). Synthetically designed storms are usually based on intensity-duration-frequency (IDF) curve. One way to generate a design storm is using the Chicago method, presented by Keifer & Chu (1975), which creates a typical CDS rain as presented in figure 2 (da Silveira 2016). The figure shows a unitless precipitation intensity on the y-axis plotted against a time of two hours. The intensity occurs at around 45 minutes in the graph, which is adjustable based on when the user wants the peak to occur. The peak shown in figure 2 is used in this project based on recommendations by the supervisor.

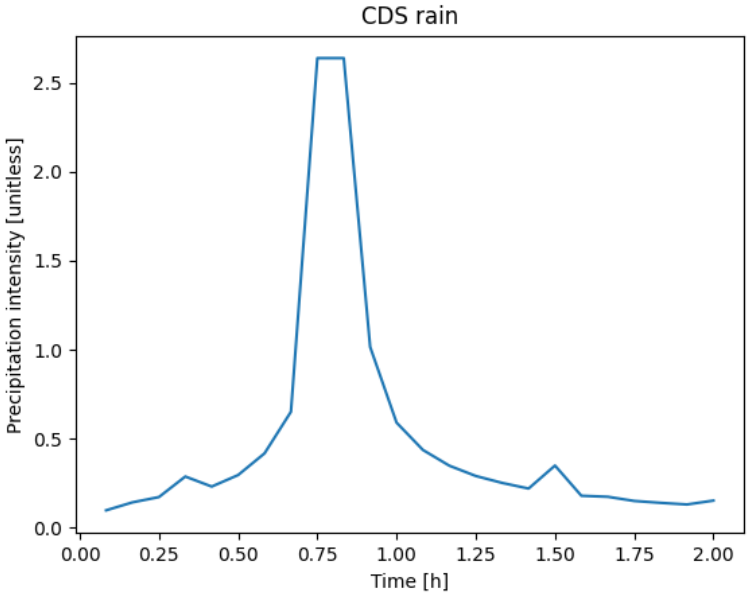

Figure 2: A typical CDS rain

2.9 Empirical hyetographs

Olsson et al. (2017) reviewed the temporal distribution of heavy rain events that have occured in Sweden based on data collected by SMHI. The rain events were then categorised by time duration of the rainfall event; $\leq$ 60 min, 60 - 90 min and $\geq$ 90 minutes. The historical events were then divided into five groups, creating five hyetographs using k - means clustering. These five hyetographs (H1, H2, H3, H4, H5) are representative of historic rain events in Sweden based on regional data and are presented in figure 3 below. According to Olsson et al. (2017), they do not occur equally common. For rain events with duration past 90 min H3 is the most common (40,1%), followed by H2 (27,3%) and H1 (18,2%) and then during more rare events H5 (8,3%) and H4 (6,1%).

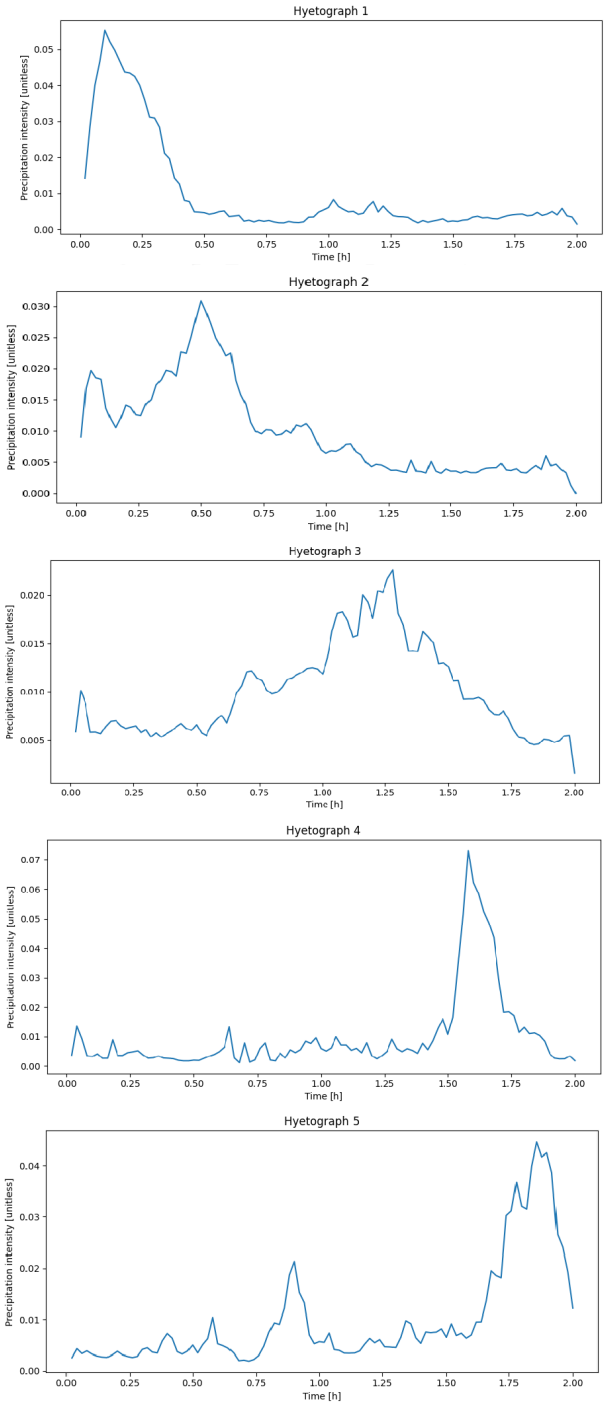

Figure 3: The five unitless hyetographs plotted against time (2h).

3 Method

The method is divided into two parts, the practical and simulation part. The practical part describes the cites, equipment and formulas used to calculate parameters through field-based experiments to determine the on-site effect of compaction. The simulations take values for parameter from previous research on similar soils as the ones chosen for the numerical simulations.

3.1 Literature study

When sourcing literature, mainly two databases were used; Google Scholar and Uppsala University's Library database. Other literature was provided by the supervisor Johan Kjellin and assistant Sara Ekeroth as well as subject reviewer Mats Larsbo. The sought after information included general soil dynamics and processes including urban flooding, soil compaction, hydraulic conductivity, compaction in agriculture and similar searches. The aim of the searches was to find information regarding the dynamics and characteristics such as infiltration in the soil when exposed to compaction similar to compaction that can occur on a urban green area. Literature that focuses on forest soil is still considered if it is relevant to the soil dynamics, for example such as at which condition the soil is most sensitive to compaction.

For information on the freeze/thaw effect in soil, Uppsala University's Library database and Google Scholar was used. The sought after information mainly revolved around the process of freeze/thaw and it's resulting effects on the soil. Search words like "freeze thaw, freeze thaw AND soil, freeze thaw AND agriculture, etc were used. The aim was to obtain information regarding the freeze-thaw process and what effect this has on the soil. Further searches such as "freeze thaw AND compaction" focused on finding information regarding how the effects of compaction are effected by frequent freeze-thaw cycles. Literature describing how the infiltration rate varies when it is flowing through actively frozen soil is not considered, as this is not focusing on the subsequent effects of the freeze-thaw cycles. Other processes were not considered as they are not relevant within the scope of this study.

3.2 Field experiments

The following chapter describes the field experiments, including the setup, laboratory experiments and calculations. Prior to conducting the experiments, the measuring station located on grass land owned and managed by The Swedish University of Agricultural Sciences (SLU)(Swedish University of Agricultural Sciences n.d.) was observed to ensure that the ground frost had fully thawed.

3.2.1 Site description

For the field experiments three urban green areas were chosen in Uppsala, Sweden. The selection process was largely based on availability and weather or not the green areas were close to some sort of parking with the possibility of using the transport car as loading weight for the simulation of compaction. The three locations are Ångström, Geocentrum and BMC presented in figure 4.

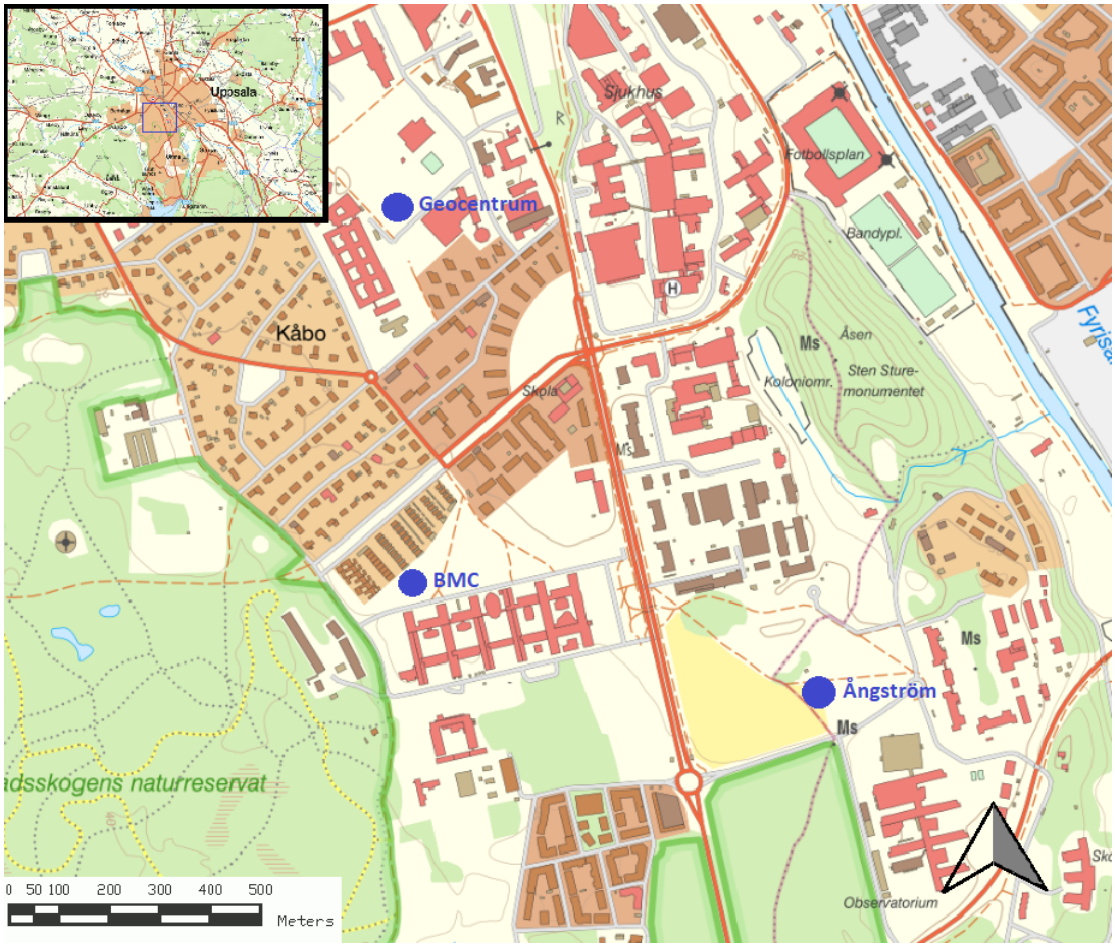

Figure 4: The three sites visualised on a map (Lantmäteriet).

3.2.2 Experimental setup

Compaction was simulated by the application of force of the rented transport vehicle used to get between sites (Toyota Yaris Cross). The vehicle is rolled back and forth on a testing area marked 20 meters in length and 5 meters in width and is estimated to weigh 1362 kg including the equipment and one driver, with a standard pressure of 2,4 bar in the tires. As seen in figure 5, a vehicle passed along side a tape measure, creating two wheel tracks. Along the tape measure are four sections marked out, divided by wooden sticks. Which section samples were taken in was randomised using an online number generator, where the numbers were 1 - 4 for each section. For each site, three sets of samples were taken on the marked testing area. Each sample set consists of three soil samples collected at 10-15 cm depth (after the initial plant cover has been carefully removed), five measurements done with a penetrologger and two infiltration measurements using a double ring infiltrometer method. A random number generator was used to determine in which section to take the measurement, to make the field measurements more statistically reliable.

The first sample set was taken on undisturbed soil, the second on soil where the vehicle had passed two times and the third when the vehicle had passed 10 times. The holes are dug in the wheel tracks after two and 10 passes. A metal cylinder used for soil sampling is hammered down into the soil and extracted using a knife, later placed in a plastic bag marked

with the sample number (figure 6). For the infiltration measurements two rings are placed inside each other, as shows in figure 7. The outer ring (25 -26 cm diameter) is used to saturate the surrounding soil, so when the water is infiltrating the soil the saturated infiltration rate is measured. For practical reasons, a plastic bucket is used as the inner ring (20 cm diameter) in the infiltration measurements. Using the proper rings (25 cm diameter inner ring, 60 cm diameter outer ring) would demand an impractical amount of water to saturate the surrounding soil.

Apart from the above mentioned sample sets, two soil samples combined with five penetrologger measurements were conducted on a part of the cite which was deemed as compacted at possible. On cite one and two this was a pathway, on cite three this was where the goal keeper usually stands during recreational activities on the green area. This sample will later be referred to as ”max”.

To avoid taking multiple samples in the same spot within the section, the penetrologger samples were taken close to the wooden stick dividers separating the sections, the infiltration measurements closer to the middle and the bulk density samples in the middle of the section as described in figure 5. It was also relatively easily visible where previous samples/measurements were taken, as the infiltration measurements left a wet spot behind and the bulk density measurements visibly disrupted the top vegetation cover.

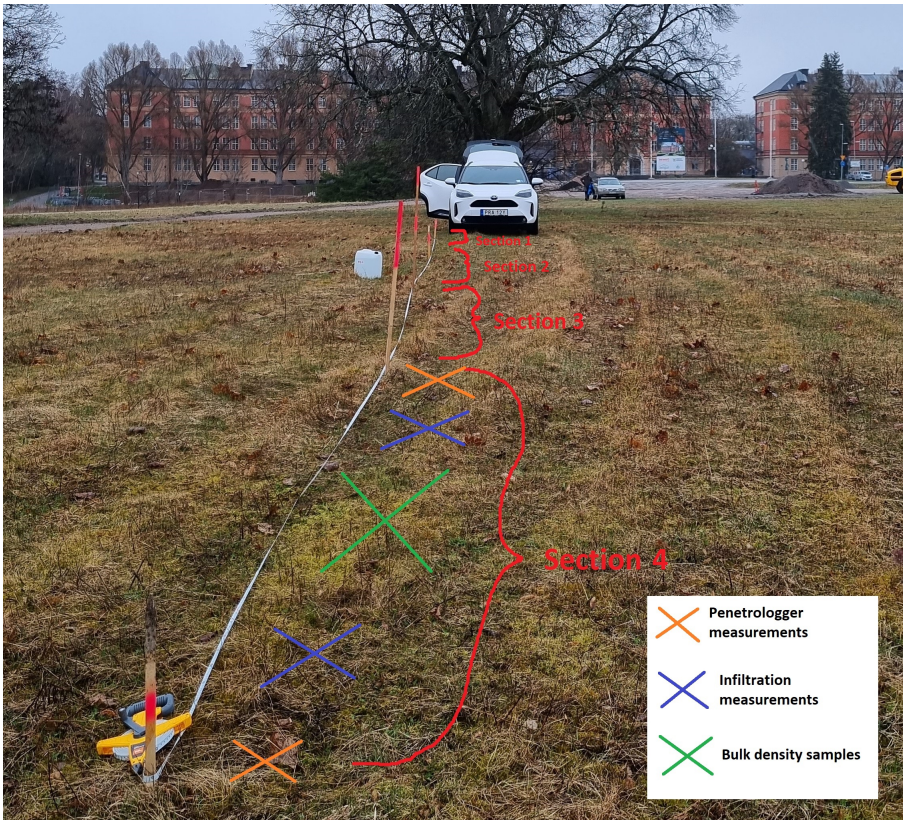

Figure 5: The testing area at one of the sites marked out. The red marks one of the sections subject to random sampling. The orange cross marks the area where the penetrologger measurements could be taken, the blue where infiltration measurements could be taken and lastly the green where bulk density samples could be taken (Photo: Anastasia Novikova).

3.2.3 Soil texture

The soil texture was determined by doing the jar test. Soil from each cite was first sieved through a 2 mm sieve to remove any larger gravel particles and to disrupt aggregate structures. The soil is then mixed with water and a little dish soap and shaken in a large glass container to properly mix the soil particles. The glass container is then left undisturbed for 48 hours so the particles can sediment. The particles sediment according to particle size, in this case sand is closer to the bottom, followed by silt and then clay on top. As the particles separated, they were differentiated by a distinct line creating visible layers. A ruler was used to determine the ratio between the three grain sizes and the corresponding soil texture was appointed from the particle size distribution classification triangle in figure 1.

3.2.4 Penetration measurements

Soil compaction measurements are made using a Eijkelkamp penetrologger provided by SLU. The apparatus was pushed down into the soil as steadily and consistently as possible. The generated values are saved on the device and extracted at a later stage. A total of 20 measurements were made on each cite; five measurements on untouched soil, five after 2 passes, five after 10 passes and five on the foothpath/goal area.

3.2.5 Bulk density measurements and moisture content

Bulk density was measured using the core cutter method. A cylindrical metal cutter was placed vertically into the soil at around 10 - 15 cm. The sample was then carefully cut out and placed in a plastic bag for further analysis in the lab, see figure 6. Originally the plan was to take a sample at 30-40 cm depth as well, but this was deemed to time consuming for the scope of this study and the appointed field days. The collected samples were weighed before and after drying at 105 degrees Celsius for 24 hours and the dry weight was then divided by the volume of the core cutter, which had a height of 4,9 cm and diameter of 7,2 cm. To determine the bulk density equation (6) below is used.

$$Bulk\ density = \frac{mass\ dry\ soil(g)}{Volume\ cylinder(cm^3)} \tag{6}$$

To get the moisture content of the soil the weight of the wet soil and dry soil after heating at 105 degrees Celsius for 24 hours is compared. The moisture content percentage is calculated according to the equation below.

$$100 - (m_{dry}/m_{wet}) \cdot 100 = \theta(\%) \tag{7}$$

3.2.6 Organic matter content

The organic matter content in the soil from each cite was measured using a further heating process, which can directly follow the drying method mentioned above. The samples, after drying, were placed in a muffle furnace at 400 degrees Celsius to burn away all the organic matter in the sample. After 4 hours, the samples were weighed again and the values noted down. The

percentage organic matter was calculated according to the equation below.

$$100 - (m_{burned}/m_{dry}) \cdot 100 = \ organic\ matter\ content(\%) \tag{8}$$

[a]  [b] 

Figure 6: Soil sample collection using the core cutter method (a - b) for bulk density measurements in the lab (Photo: Anastasia Novikova)

3.2.7 Infiltration measurement

The infiltration rate of the soil was measured using the double ring infiltrometer method. Two rings with diameters 25 and 20 cm were pushed down into the soil using a hammer. The inner ring used was not made out of metal, but was cut out of a plastic bucket. Due to the fragile state of the plastic bucket, it could not be hammered down as easily as the metal outer ring, and the soil underneath the bucket edge had to be cut using a knife to make room for the plastic ring. Water is then poured into the outer ring to saturate the surrounding soil before pouring water into the inner ring. The rate at which the water level decreases in the inner ring is measured using a ruler and a timer, noting down the water level in mm after each minute passed, until a steady state is reached when the level decreases at the same rate between each minute. The same water level is kept in the outer ring as in the inner, to ensure a constant pressure. See figure 7 for the setup. When the infiltration rate has reached a steady state, the measured value is said to equal the hydraulic conductivity of the soil (Reynolds et al. n.d.).

For the bulk density samples, penetrologger measurements and the infiltration measurements; a t-test was conducted to see if there is a significant difference between the obtained data sets for 0, 2, 10 vehicle passes as well as the pathway which is referred to as the ”max”.

Figure 7: Infiltration measurements setup (Photo: Anastasia Novikova)

3.3 Soil simulations

When choosing soils and their respective parameters, information was collected from different studies where ever the needed information was available. Very few studies measured all the necessary parameters for the simulations, Therefore many soils have, for example, gotten their bulk density value from one study and their soil texture from another. This is due to the fact that few studies are available where all the necessary parameters for the simulations are measured. When available, studies focusing on urban green areas are used. Where the necessary information was not available, assumptions were made based on existing available information for remaining soils.

3.3.1 Soil particle composition

Five soils are chosen with varying particle size composition for the Rosetta program. The five soils are aimed to represent different extremes of urban green areas that can be found in figure 1. Two of these soils are based on recommendations by AMA Anläggning (2020) and RA Anlägging (2020) technical handbook for park landscaping. They include a *sandy loam* (15 % clay, 25 % silt, 60 % sand) and a *loamy sand* (5 % clay, 15 %silt, 80 %sand) type soils. A *sandy* soil (2,05 % clay, 4,29 % silt, 93,66 % sand) was chosen based on measurements done on lawn soils by Duan et al. (2011). A *silt loam* soil (23 % clay, 63 % silt, 14 % sand) was chosen based on measurements done on residential lawns in Pennsylvania (Hamilton & Waddington 1999). Lastly,

a *clay* soil (63,68 % clay, 12,63 % silt, 23,69 % sand) is chosen based on measurements done by Lan et al. (2019) on a park lawn in Taifeng Park, China. The clay soil, unlike the others, has specified soil texture composition in both the upper 0 - 10 cm as well as at 20 - 30 cm. Although the composition percentages slightly changed, the soil still remained classified as a clay. Based on this, it is assumed that the soil texture remains the same in both upper layers and lower layers for all soils.

3.3.2 Bulk density

Bulk density (ρ_d) was only measured in the studies conducted on the clay and silt loam soil and bulk density in the deeper layer was only measured for the clay soil. Remaining bulk densities are based on different studies where the same soil classification is identified. Both the bulk density and the bulk density in the lower layer on a loamy sand was based on a study conducted by Osunbitan et al. (2005) where the effect of tillage on bulk density was evaluated. The bulk density for the sand soil is given by Gregory et al. (2006), for the clay it is provided by Lan et al. (2019) and the silt loam bulk density is based on the residential lawns in Pennsylvania mentioned above.

3.3.3 Bulk density change with depth

The bulk density in lower layers are given for the clay and silt loam, and the value is increased by 13% and 8% respectively. For a similar depth increase for other soils, the bulk density is set to increase with the mean value of 10,5% in the lower layers for the sandy loam, sand and silt loam.

3.3.4 Bulk density change with compaction

Variations in soil bulk density is known to change due to compaction of different degrees. Due to lack of research on urban lawn soil compaction the change in bulk density for different soils is based on measurements done on mainly pastures and agricultural land. Gregory et al. (2006) measured that an application of weight for 10 minutes resulted in a bulk density increase from 1,49 to 1,73 g/cm^3 (16% increase) on a pasture site containing over 90% sand when using a handheld steel plate vibrating compactor. Similarly, for coarse grained soils containing around 60% sand, the bulk density increased between 16 - 25% when exposed to a single pass of grain harvesting equipment (Ansorge and Godwin 2007, Antille et. al 2013 see Ngo-Cong et al. (2021)). Cotton harvesting equipment passing on small grained soil containing 50 - 70% clay, showed an increase in bulk density of 6 - 15% (Antille et.al 2021 see Ngo-Cong et al. (2021)). Bulk density measurements conducted on a silt loam pasture during post-grazing showed an increase of 15% in bulk density on the upper layer (0- 10 cm) (Hu et al. 2018).

With increasing compaction, the current bulk density will start nearing the maximum bulk density at present conditions. Therefore it is not realistic that the increase in bulk density of the subsoil layer occurs at the same rate as it does closer to the surface. When measuring the effect of compaction on a pasture site in New Zealand Hu et al. (2018) found that the effect of compaction was slightly less in layer 10-20 cm, 5,2% compared to the 12% bulk density increase in the top 10 cm layer. Based on this, the bulk density increase will be estimated to change at half the rate

for remaining soils in the subsoil layer at 30-40 cm.

A summary of the above mentioned parameters and change in bulk density for each soil is presented in table 1.

Table 1: Change (Δ) in bulk density (ρ) at different degrees of compaction for sandy loam (A), loamy sand (B), sand (C), clay (D) and silt loam (E) both in the upper and lower layer, given in percentage and g/cm^3.

Tag	Δ top layer (%)	ρ top layer (g/cm^3)	Δ bottom layer (%)	ρ bottom layer (g/cm^3)
A0	0	1,37	0	1,51
A1	9	1,49	5	1,58
A2	17	1,60	9	1,65
A3	25	1,71	13	1,7
B0	0	1,3	0	1,4
B1	9	1,41	3	1,44
B2	17	1,52	9	1,52
B3	25	1,63	13	1,57
C0	0	1,49	0	1,65
C1	6	1,58	3	1,7
C2	12	1,67	6	1,74
C3	16	1,73	8	1,78
D0	0	1,39	0	1,57
D1	5	1,46	3	1,61
D2	10	1,53	5	1,65
D3	15	1,6	8	1,69
E0	0	1,02	0	1,12
E1	4	1,06	1,7	1,15
E2	8	1,10	3,5	1,17
E3	12	1,14	5,2	1,18

3.3.5 Rosetta

For the theory based soils, their predetermined soil composition of sand, silt and clay as well as bulk density will be provided as inputs to Rosetta. The program will then estimate the residual soil water content θ_r, saturated soil water content θ_s, saturated hydraulic conductivity Ks, the inverse of entry air pressure α and the pore size distribution n (United States Department of Agriculture n.d.*a*).

3.4 HYDRUS-1D model

The model to simulate the soil infiltration during rain events was originally supposed to be done in the HYDRUS-1D Graphical User Interface, but was later executed in Phydrys, which is the Python implementation of the HYDRUS-1D model due to the large number of simulations. This program was chosen due to it being used in similar reports (Hilten et al. 2008). The soil profile

created was divided into two layers, the first layer spanning from the surface down to 15 cm and the next layer spanning between 15 down to 40 cm. The hydraulic soil processes in the profile are based on the van Genuchten Mulaem single porosity model. For the root water uptake Feddes water uptake reduction model was chosen and the default parameters provided by HYDRUS remain unaltered for the simulations. Evapotranspiration was neglected in the model as the simulated rain events had a short time span (2 hours) compared to e.g simulations of historical rain series.

The upper boundary condition was set to "Atmospheric BC with surface runoff" where the excess water is simulated as surface runoff when the water flow into the soil is higher that the infiltration capacity. The bottom boundary condition was set to constant pressure head and the groundwater table was set to start at one meter, and was later changed to two meters due to it being a more realistic groundwater level. Observation nodes are placed at 10, 20, 30 and 40 cm depth in the soil profile. The resolution of the soil profile is set to measure every 0,05 m, which is the size of each grid cell. This was done apart from simulations where the numerical solution did not converge. In that case the resolution is increased to 0,04, which is the limit.

3.4.1 Rainfall simulation

The length of each rain event was set to two hours and is based on empirical hyetographs H1 - H5 mentioned in figure 3. The volume of each extreme rain event is based on an online statistical tool provided by the Swedish Meteorological and Hydrological Institute (SMHI) (*IDF SMHI* n.d.). The online tool can provide both volumes based on historically measured rainfall but also for different climate scenarios. In this report, only volumes based on historical rain fall is simulated. Sweden is divided into four regions and for these simulations, the south east is chosen. The volume is dependant on the return period of the rain event and the chosen return periods were 2, 10 and 100 years. Table 2 shows the volumes used.

Table 2: The rainfall amount used in the simulations for a 2, 10 and 100 year cloudburst event.

2 years	10 years	100 years
19,5 ± 0,5 (mm)	28,2 ± 1,6 (mm)	47,4 ± 7,5 (mm)

These volumes are then multiplied with H1 - H5 and that gives the correct rain fall amount and distribution used in the simulations.

4 Results

4.1 Field measurements

4.1.1 Site description and Soil texture

Site 1 (Ångström):
The samples taken and experiments conducted on the Ångström site were during a rainy day, so the soil had been partially saturated. The vegetation cover consisted of medium length grass and the area had moss partially grown over it. The area had varying composition which was noticed when samples were taken in the pathway, that had a large amount of gravel mixed in. Construction work has been conducted close to this site for many months, but the sampling area selected was located significantly further away.

Site 2 (Geocentrum):
This urban green area consisted of short grass and the exact location where the samples were taken the vegetation cover also had moss partially growing on it. The area is regularly used for recreational activates but the chosen sampling area was along side a bush at the outskirt of the site to ensure that the soil was as undisturbed as possible.

Site 3 (BMC):
A significant amount of garden waste consisting of branches, logs and leaves were located close to the chosen sampling area, which indicates the use of machine traffic. A construction site is also noted about 200 meters from the sampling site but is deemed to be negligible. When digging quite many earthworms as well as multiple ant nests were found and carefully removed from the soil if a sample was to be taken there.

The soil texture composition is presented in table as a result of the jar test.

Table 3: Soil texture for the three measured sites; Ångström, Geocentrum and BMC

Site	Clay (%)	Silt (%)	Sand (%)	Texture
F: Ångström	1,92	23,08	75	Loamy sand/ Sandy loam
G: Geocentrum	0	23,29	76,71	Loamy sand
H: BMC	1,33	18,67	80	Loamy sand

All soils tested are according to the jar test very high in sand content and low in clay content, similar to the AMA soils which are mentioned as ideal for urban landscaping projects.

4.1.2 Bulk density, moisture content and organic matter content

The average of the three bulk density measurements and their standard deviation for each site after each pass is plotted and presented in figure 8.

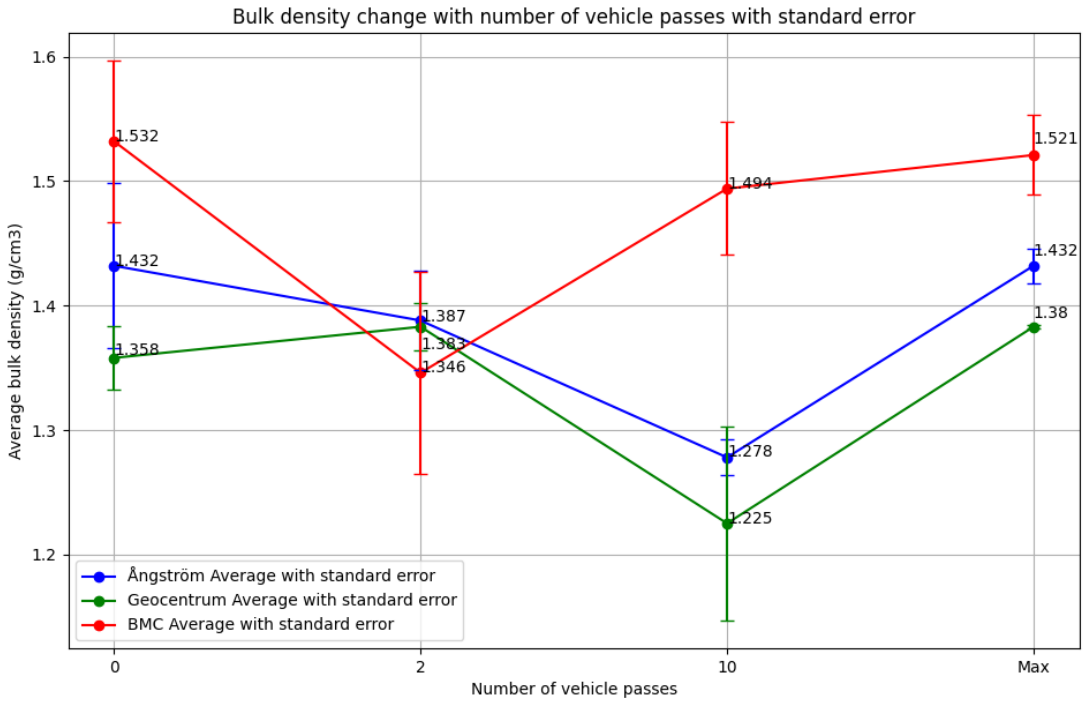

Figure 8: Change in bulk density with number of vehicle passes as well as the pathway measurements ('max') for the three site locations: Ångströms, Geocentrum and BMC, with standard error.

The results show that no clear linear correlation can be identified between number of vehicle passes and change in bulk density for any of the sites, despite visible wheel tracks after both 2 and 10 passes. For the BMC site the beginning bulk density value even exceeds the supposed maximum compaction value taken in a walk pathway and it is also the soil containing the highest fraction of sand, which typically would result in a lower bulk density. The t-test could not determine if the bulk density samples are significantly different, for specific p-values, see Appendix B.

An average of the soil moisture content from all the samples taken from each site is calculated and presented in table :

Table 4: Soil moisture content for each site

Ångström	Geocentrum	BMC
14,26 (%)	19,92 (%)	16,08 (%)

The highest moisture content is observed at Geocentrum at almost 20% followed by BMC at 16,08 % and lastly Ångströms at 14,26 %. The samples from Ångströms were taken during a day that experienced raining throughout the day, but had the lowest moisture content.

An average of the organic matter content from all the samples taken from each site is calculated and presented in table :

Table 5: Organic matter content for each site

Ångström	Geocentrum	BMC
4,25 (%)	5,89 (%)	4,58 (%)

The highest organic matter content is observed at Geocentrum at almost 6% followed by BMC at 4,58 % and lastly Ångströms at 4,25 %.

4.1.3 Infiltration measurements

The 2 - 3 infiltration measurements done after each pass and cite are averaged and presented in figure 9.

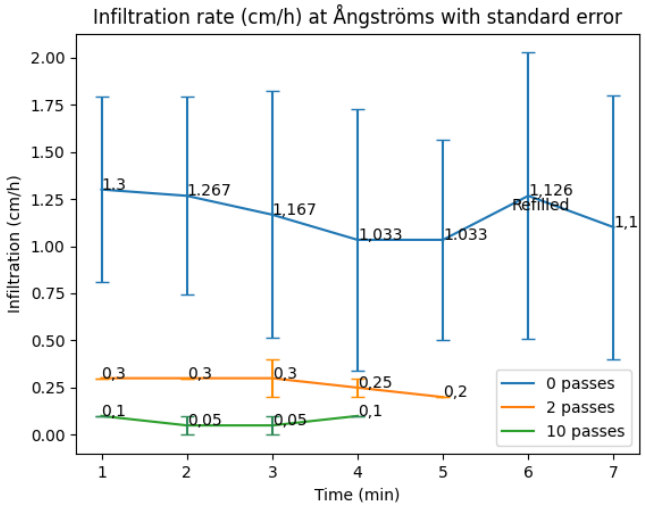

[a]

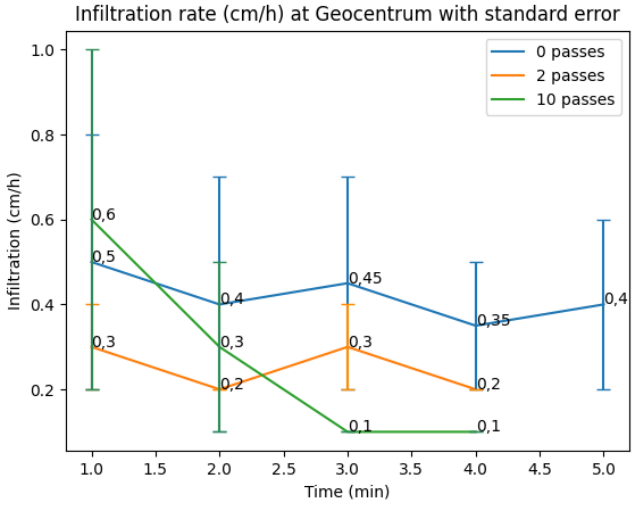

[b]

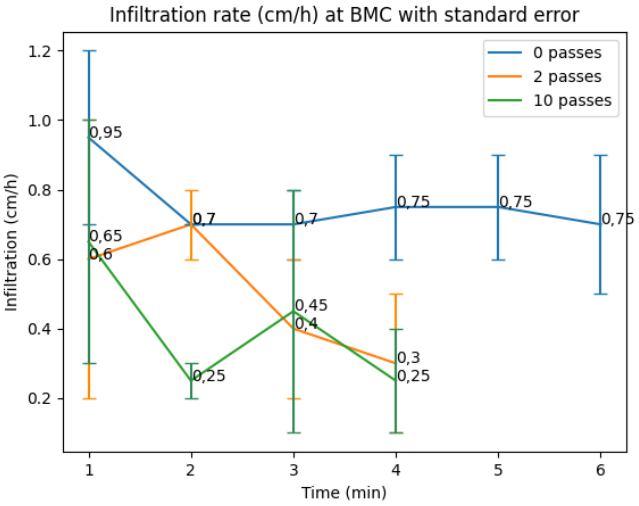

[c]

Figure 9: Change in infiltration rate with each measured vehicle pass at the three sites a) Ångström, b) Geocentrum and c) BMC shows with standard error.

In some instances the measurements are cut short, and the infiltration rate has not yet reached steady state, which should be the last measured value. Despite this, a clear correlation can be made. In all three figures a clear trend is observed as the infiltration rate decreases with the number of vehicle passes increases.

4.1.4 Cone Index penetrologger measurements

Figure 10 shows the measure cone index values taken with the Eijkelkamp penetrologger on each site. The five measurements done after each measured vehicle pass on each site is averaged and plotted against each other in three figures corresponding with the site.

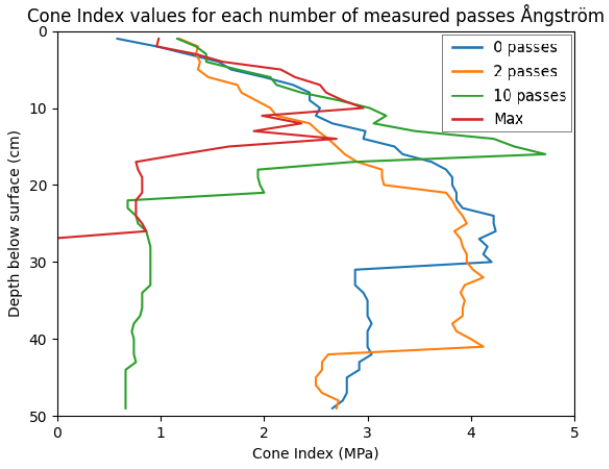

[a]

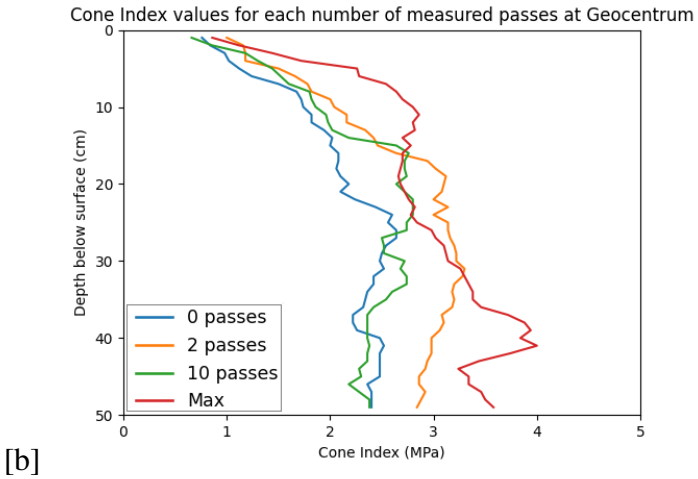

[b]

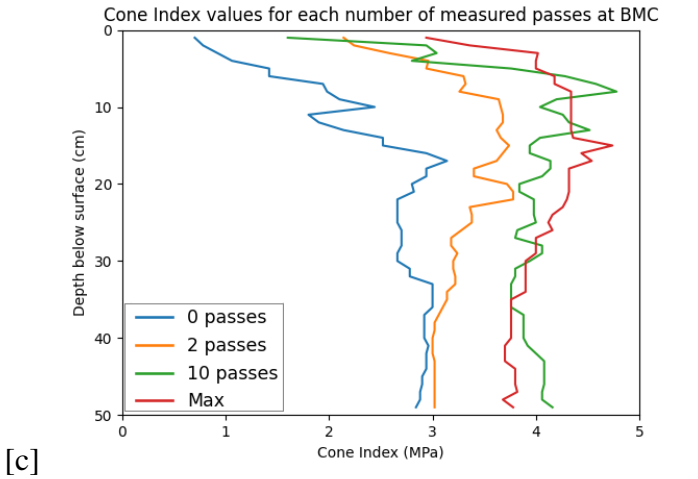

[c]

Figure 10: Cone index values for the sites Ångström (a), Geocentrum (b) and BMC (c) after each measured number of passes (0, 2, 10) including an additional measurement done in a close by pathways labeled as "max".

The best obtained measurements with the clearest correlation with level of compaction was obtained at the BMC site, plot c) shows a clear increase in kPa with increasing number of vehicle passes, with the largest resistance being in the pathway located close to the sampling site. Throughout almost the whole measured soil profile, the Geocentrum site b) also shows that the pathway location 'max' had the heaviest resistance and the untouched soil (0 passes) the least resistance. b) and c) Therefore indicate that continuous foot traffic is a cause for compaction. Site Ångström a) showed unclear results as seen in the figure, the best measurements could be obtained for 0 and 2 passes, whilst the measurements for 10 passes and 'max' are inconsistent and jagged. When looking at their values for the first 15 cm of the soil profile the results look promising, reaching 3 - 4 kPa. After that they show very low values. It was also noted during the field measurements at this site that pushing the penetrologger into the soil was more difficult that previous sites. When measuring in the pathway at the Ångström site the pentrologger could not be pushed further down than 30 cm, most likely due to different material below this depth.

The t-test results are presented for three separate layers from 0-10 cm, 10 - 30 cm and 30 - 50 cm. If the obtained p-value is below 0,05 then the data sets are considered significantly different from

each other. The specific p-values are shown in Appendix B.

The test results showed that for the top layer (0 - 10 cm) the only soils that had a significant difference at Geocentrum were the comparison between 0 and "max" number of passes. For BMC all soils (2, 10 passes and max) showed a significant difference with 0 passes. At Ångströms the top layer for 0 passes showed no significant difference with any of the soils. Generally the significant difference increases for all sites with depth, both for the 10 - 30 cm layer as well as the 30 - 50 cm layer. For specific p -values, see Appendix B.

4.1.5 Limitations

Due to the unexpected results obtained for the bulk density measurements, they could not be inserted in Rosetta to obtain the changing soil parameters to then be inserted in HYDRUS-1D and modelled with the hyetographs. This was due to no increase in bulk density was noted after manual compaction with the Toyota Yaris Cross vehicle. As previously mentioned, two ways to measure compaction is either through bulk density increase or penetration resistance measurements. To be able to obtain the hydraulic parameters from Rosetta for the HYDRUS model, a change in bulk density is necessary if one wishes to simulate a runoff from a changing soil profile with compaction. There is no possibility to enter penetration measurements into the Rosetta program and therefore no simulations in HYDRUS were made based on parameters obtained in the field, despite this being the ambition at the start of the project. Therefore, the dual method approach mentioned in the aim, could not be implemented and compared, but it was still possible to highlight insecurities with the two methods.

The results for the bulk density measurements obtained from the field experiments were not as expected, but the numerical simulations are still conducted. This is due to there still being a visible change on both infiltration and some of the penetration resistance measurements as well as supporting literature.

4.2 HYDRUS-1D simulations

All the soils mentioned in table 1 have been run through the model for H1 - H5 and 2, 10 and 100 year return periods as well as the CDS-rain for the same return periods. Each section is plotted in graphs for each degree of compaction resulting in a total of 90 plots for the different combinations. Below follows a few of the simulated plots in figure 11. The legend in the plots notes the different levels of compaction for the upper and lower level divided by a dash.

The simulations for the 100 year CDS rain show the different soils react with increasing compaction. A clear pattern is seen in almost all the plots, where the amount of runoff increases with increasing compaction. The anomaly in these simulations is the silt loam, where the second degree of compaction (E2) is not plotted due to non-convergence which was consistent for all simulation scenarios. No runoff occurred on the sand soil and is therefor not shown in figure 11.

To better quantify the relation between the amount of runoff in relation to precipitation amount, a runoff coefficient is used as described in equation (9).

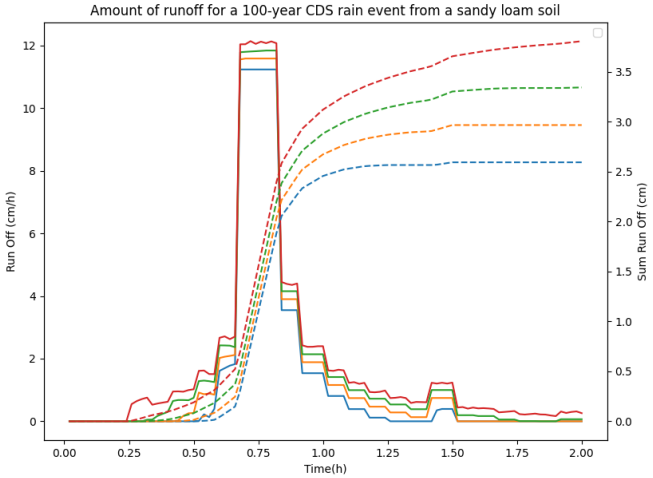
Amount of runoff for a 100-year CDS rain event from a sandy loam soil
Run Off (cm/h)
Sum Run Off (cm)
Time(h)

[a]

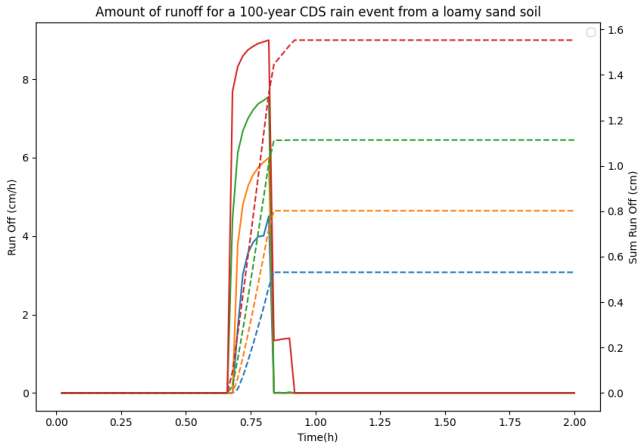
Amount of runoff for a 100-year CDS rain event from a loamy sand soil
Run Off (cm/h)
Sum Run Off (cm)
Time(h)

[b]

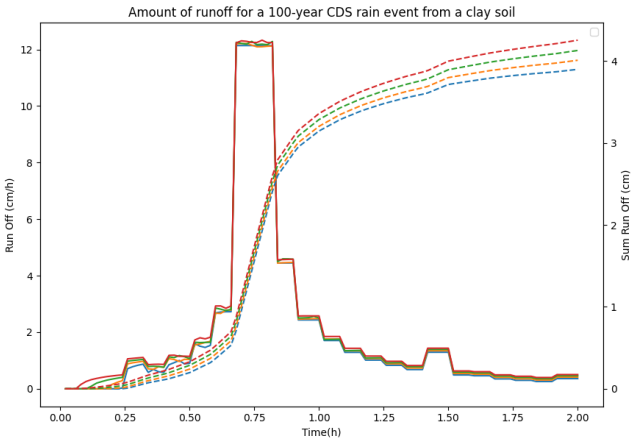
Amount of runoff for a 100-year CDS rain event from a clay soil
Run Off (cm/h)
Sum Run Off (cm)
Time(h)

[c]

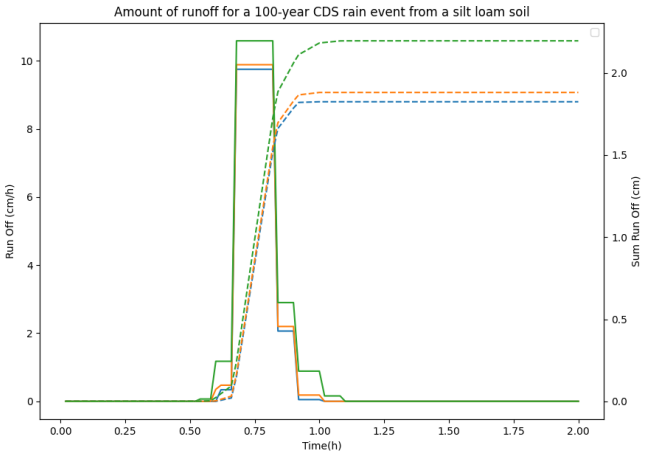

[d]

Figure 11: The five soils at each compaction degree simulated against a 100 year CDS rain where a) sandy loam, b) loamy sand, c) clay, d) silt loam. The blue line represents no compaction, the yellow is the first degree of compaction, the green is the second degree of compaction and red is the third and most compacted scenario. Except for plot d) silt loam, where the green is the third degree of compaction as the second degree could not be plotted.

$$Runoff\ coefficient = \frac{Runoff\ (cm)}{Precipitation\ (cm)} \tag{9}$$

A summary of all the simulations are presented in figure 12 where the runoff coefficient is noted, sectioned and color coded. Each of the soil types are referred to as A (sandy loam), B (loamy sand), C (sand), D (clay) and E (silt loam). The number next to each level denotes the level of compaction which was specified in table 1. The black cells are simulations that could not converge during the simulation, resulting in a lack of a numerical result. Values closer to 0 indicate that a small amount of the precipitation ended up as runoff, values closer to 1 indicate that the a majority of the incoming precipitation ended up as surface runoff.

Summary of all the simulations

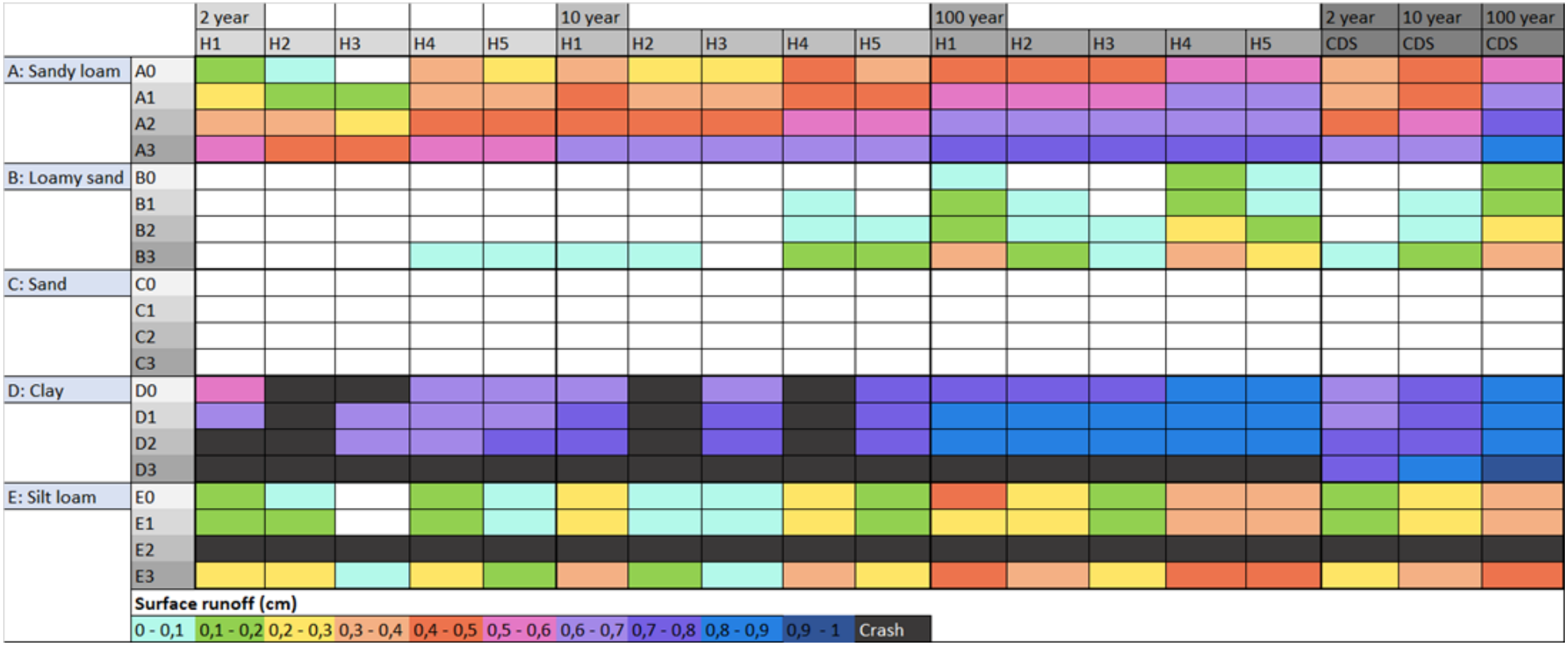

Figure 12: Runoff coefficient for each type of soil, degree of compaction, hyetograph and 2,10 and 100-year rain

The results from the simulations show a clear pattern that the amount of runoff increases with increasing volume of rain, the runoff also increases with the amount of compaction for almost all soils. Further analysis shows that the clay soil has generally the highest runoff for all simulations, followed by sandy loam, loamy sand and lastly the sand soil with no runoff for any of the simulations. A clear difference can be seen between the the hyetographs when looking at the sandy loam simulations. There is a higher runoff for H4 and H5 with later peaks, followed by H1 and then H3 and H2 for the 100 and 10 year cloudbursts.

Based on these simulations, a clear parallel can be drawn between the amount of sand a soil has and the amount of runoff. The sandy loam (A0 - A3) and loamy sand (B0 - B3) are two categories similar in composition, but the loamy sand contains more sand (80%) compared to the 60% that the sandy loam has. The highest percentage is in the sand soil with 93,66%. We see the amount of runoff decrease for each soil with increasing sand concentration, ending in zero runoff for the sand soil for all the simulations.

When comparing the runoff from the CDS rain events with the hyetographs, both the runoff amount as well as pattern in regards to runoff change with compaction is most similar to H4, despite them having different peaks.

If the hyetographs are weighed against each other according to how common they are, as described in section **2.10**, one average precipitation hyetograph is produced for 2, 10 and 100 year cloudburst events, denoted as simply ”H”. The hyetograph is shows in figure 13. The simulations are run again for the averaged hyetograph H and presented in figure 14

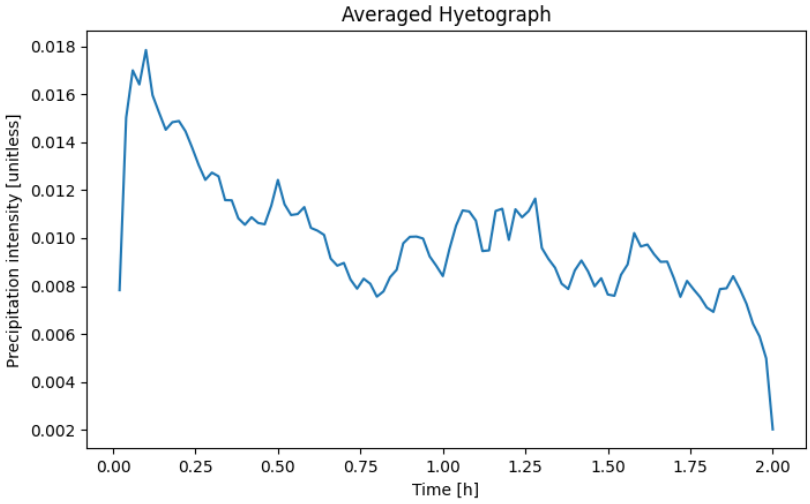

Figure 13: Averaged hyetograph

		2 year	10 year	100 year
		H	H	H
A: Sandy loam	A0		0,05	0,38
	A1	0,02	0,24	0,53
	A2	0,20	0,43	0,65
	A3	0,46	0,63	0,78
B: Loamy sand	B0	0	0	0
	B1	0	0	0
	B2	0	0	0
	B3	0	0	0
C: Sand	C0	0	0	0
	C1	0	0	0
	C2	0	0	0
	C3	0	0	0
D: Clay	D0	0,52	0,67	0,81
	D1	0,59	0,72	0,84
	D2		0,77	0,87
	D3			
E: Silt loam	E0	0	0	0,03
	E1	0	0	0,04
	E2			
	E3	0	0,0011	0,18

Figure 14: Runoff coefficient for each type of soil, degree of compaction for the averaged hyetograph.

The values from 14 are plotted against degree of compaction for the sandy loam soil and presented in figure 15 and 16 for the clay soil corresponding with the compaction scenarios A0 - A3 and D0 - D3. Sandy loam and clay are chosen from the figure above due to having the most consistent results.

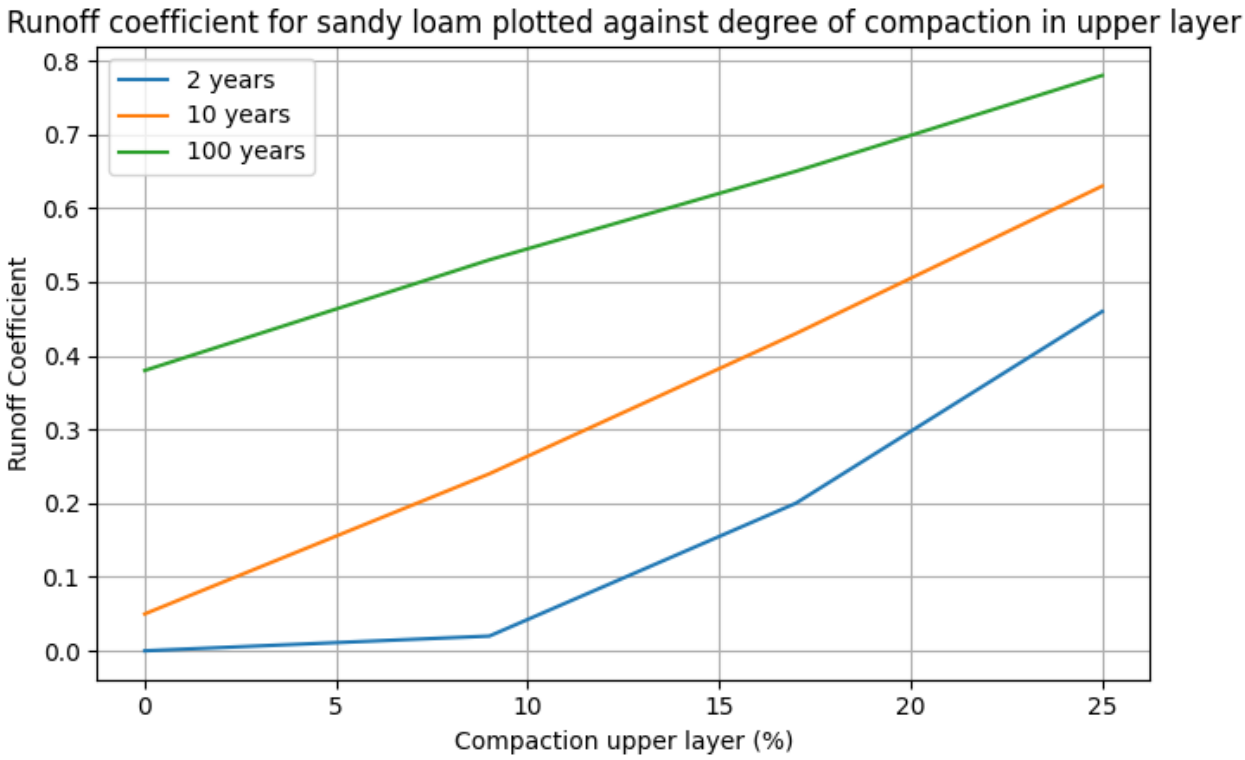

Figure 15: Runoff coefficient plotted against degree of compaction for the three averaged hyteographs (2, 10 and 100 year) for sandy loam soil

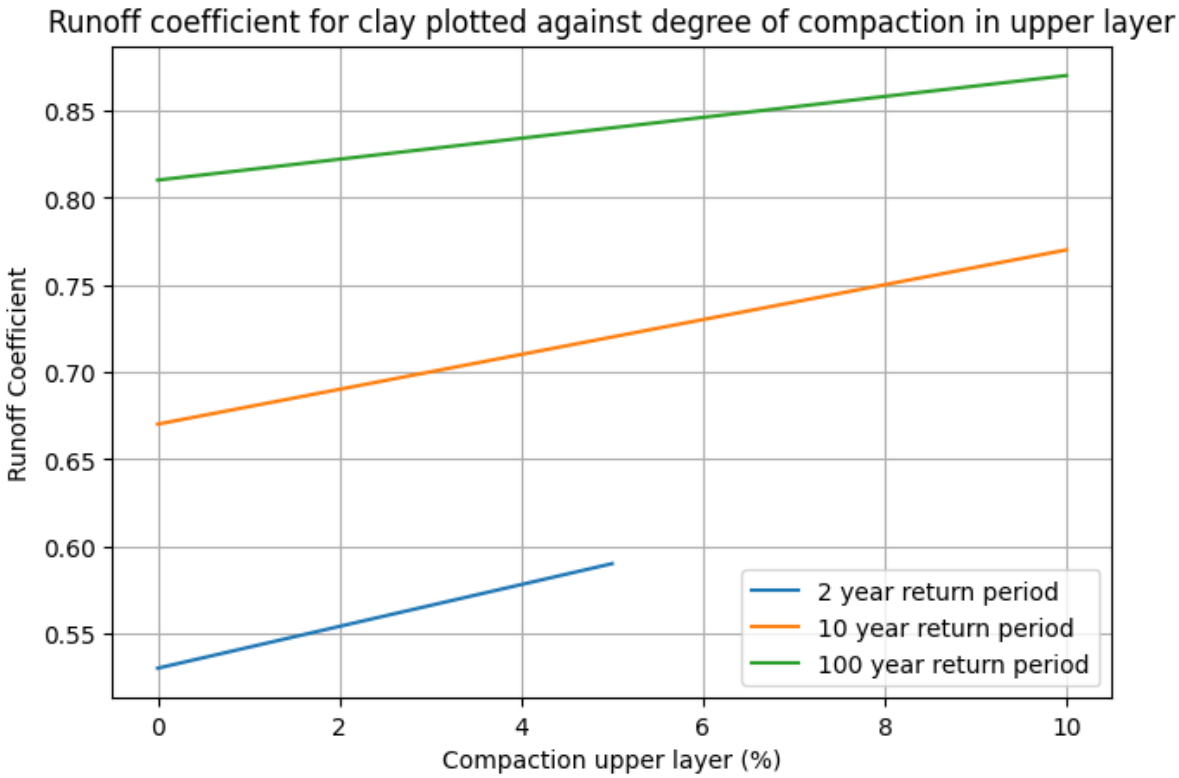

Figure 16: Runoff coefficient plotted against degree of compaction for the three averaged hyteographs (2, 10 and 100 year) for a clay soil

There is a clear correlation between the runoff coefficient and compaction for both the sandy loam and the clay soil, but what differentiates them is that sandy loam is more sensitive to compaction than the clay soil. This can be seen when comparing figure 15 (sandy loam) and figure 16 (clay) as the increase in runoff coefficient is changes more rapidly for the sandy loam than clay. The runoff from the clay soil are generally higher than for the sandy loam,

5 Discussion

5.1 Field measurements

During the field experiments, two ways of measuring soil compaction were evaluated; bulk density change and cone index. The bulk density measurements taken on the sites showed unexpected results as no clear increase in bulk density was noted after each number of measured vehicle passes. Looking at the raw data from the lab measurements (Appendix A), one can see that the bulk density have a large variation, and in the instance that one of the three values are very high, then the average is significantly increased. This result shows the heterogeneity of the soil and that three samples are possibly not enough to get a proper average of the soil bulk density. Another large factor can simply be that the vehicle used was not heavy enough to compact the soil significantly at the depth where the samples were taken. The studies referred to for the soil composition used in the simulations have been exposed to larger vehicles that are commonly used in agriculture. Although Pulido-Moncada et al. (2019) noted that multiple passes with a lighter vehicle resulted in more compaction than a single pass with a larger and heavier vehicle, the weights are still 8 ton and 12 ton respectively, which is more than double of the 1362 kg vehicle used in the field experiments. The same study already found minor effects when using a 3 ton vehicle compared to the 8 ton vehicle. Although these results were unexpected, the study by Gregory et al. (2006) found a change in bulk density when the soil was compacted by heavy machinery, Therefore the different results are mainly attributed to the relatively light vehicle used. There is also the possibility that the soils tested in the field experiments were already at a certain level of compaction prior to the field experiments due to extensive use in the past. This would make the soil less likely to compact further when the vehicle used is of the lighter variety. Some of the samples tested showed bulk densities in the 1,5 - 1,6 range, which is significantly higher compared to what typical sandy soils have (Rai et al. 2017). If this is the case, it further emphasizes the need of proper management to avoid further compaction over time. It also opens up for further studies regarding how effective the freeze-thaw effect is at restoring the soil to conditions prior to compaction.

The other way to measure compaction is with the help of a penetrologger which in this project gave mixed results. A clear relation between number of passes and pressure can be seen for the BMC site, indicating that the vehicle passes had significant effect on both the surface layer and even in deeper layers. The same cannot be said for Geocentrum where the change was minimal, but in deeper layers there is a clear difference between 0 passes and the max-value, indicating a possibly permanent compaction in lower layers that was there prior to the field visit as the max-mesurement was taken in a pathway. The values from the Ångström site are inconsistent and show no correlation, most likely due to the wet soil and unknown underlying material. Multiple readings during the field day had to be redone due to tough soil resistance, rocks and uneven penetration.

The exact value for the measured infiltration might not be a proper representation of the soils saturated hydraulic conductivity as measurements sometimes were cut short due to time restraints and had not enough time to reach the realistic steady state. No conclusion can be drawn whether or not the infiltration rate at deeper layers is affected as this was not sampled. Although not confirmed in this study, (Yang & Zhang 2011) found a clear correlation between increasing bulk

density and decreasing infiltration rate in the event of urban soil compaction. As seen in figure 9, a clear difference can be seen in the infiltration rate for all sites at the surface layer and indicate that even a proportionately light vehicle like the Toyta Cross has an affect on the infiltration rate at the surface layer. The same results were obtained by Gregory et al. (2006). Although a significant decrease in infiltration, as mentioned before, the compaction may not be permanent. This is due to the soil being able to restore itself to some degree, with a higher restoration rate the lighter the applied force. In the event of the infiltration rate becoming lower than the rainfall intensity, there is a significant risk of runoff. Therefor it is vital to uphold sufficient urban environment management as more intense rainfall events occur. Situations where the soil is rendered more vulnerable to compaction, such as during rainfall at a construction site where heavy vehicles are used, should be avoided.

It is established that contact pressure is the cause of compaction in the topsoil, whilst axle load is the cause of compaction in the subsoil. Contact pressure can also be described as weight per contact area. For reference, an axle load of 5 tonnes is not very likely to cause subsoil compaction (Duiker 2005). There is no clear reason as to why the results showed such a good correlation for the BMC site, as the moisture content as well as organic matter content was similar for all sites. As a general improvement increasing the tire size and using more light-weight vehicles would be a way to reduce the risk of compaction (Håkansson & Petelkau 1994).

Generally it is impossible for the bulk density samples, penetrologger measurements and the infiltration measurements to be taken in the exact same spot, as the soil structure is instantly changed as soon as one sample is taken. This can cause for example that one infiltration measurement for 0 passes is conducted on a spot with dense soil and a measurement for 10 passes be conducted on a spot with multiple macro pores resulting in uncorrelated values. This is a inevitable issue when taking measurements in the field and the varying results from the field measurements in this study shows how heterogeneous the soil really is.

Furthermore, as the bulk density measurements were unexpected, they were not able to be used in the HYDRUS-1D simulations. This meant that any potential change in runoff amount correlated to the sites' soil moisture content or organic matter content were not able to be compared or evaluated. The latter of which is known for to significantly affect the bulk density and the soils ability to withstand the effects of compaction (Maynard (2000) see Burghardt & Schneider (2018)) by increasing infiltration, even more so than tilling (Olson et al. 2013).
It is also worth noting that the jar test resulted in a surprisingly low clay content for all three sites, which is deemed a bit unrealistic and can only allot to human error or that the top layer of the soil has been filled with a more sandy soil many years prior during the allocation of the urban green area. The same sites were sampled and the respective soil texture measured using the jar test by Nilsson (2023). His study found that the underlying layer (30 cm) contained a much higher percentage clay (around 20% for all three sites). This reinforces the possibility that the sites soil composition has been altered to contain more sand, as Uppsala is known to have a high clay content in the soil (Fryksten & Nilfouroushan 2019). The measured soil textures should Therefore be taken as an estimate.

5.2 Modelling analysis

As seen in the visual summary of all the simulations, the simulations for the third degree of compaction for the clay soil (D3) cannot run and instead crashes, not producing any out-files. This is a known problem to happen when the model has too unrealistic parameters as noted by the creator of the software (*Hydrus-1D Forum* n.d.). The runoff is significantly higher for the clay soil in general, and is most likely quite sensitive to large amounts of water infiltration the profile, therefore it is not unreasonable that the simulation crashes. It is also worth noting that when the model was ran against a groundwater level at 1 meter depth, there were only 4 crashes in total, compared to the 44 crashes when the groundwater level is set to 2 meters down in the soil profile. The latter is still considered more realistic and these simulations were therefore kept as the final result. The issue related to the crashes could also be related to the software's unfamiliarity to the model, and not the ground water level itself.

A one meter groundwater level was seen as unrealistic and therefore changed to 2 meters, which generally gave less runoff when comparing the out-files. The sandy loam and loamy sand soils were initially run in 0,05 m resolution and then the model experienced difficulties when running for the clay, Therefore the resolution was changed to 0,04 m and this setting was run through the rest of the model (for clay and silt loam). After going back and running sandy loam, loamy sand and sand through 0,04 m resolution they crashed and experienced other difficulties, so the values for 0,05 m resolution is kept. When comparing the runoff amount for 0,04 m and 0,05 m resolution the difference was minimal, so it was not deemed as significant. The difference between 0,5 m and 0,05 m resolution is greater and could even give different results as in runoff/no runoff.

Assuming that the soil texture is homogenous throughout the profile is a possible source of error as that is not always the case. This was shown by Nilsson (2023) when sampling urban green areas in Uppsala. His measurements showed that two loamy sand topsoils had a sandy clay as well as a sandy loam subsoils. As mentioned in the theory, having a higher percentage of sand in the lower layer could improve drainage and a more clay-rich layer could hinder it, leading to varying results.

The simulations in general showed correlating results with higher runoff for increased degree of compaction as well as higher runoff for the clay soil and less runoff for soils with higher sand content. Higher runoff for H4 and H5 is most likely due to the later peaks, which means that the soil is already saturated when the peak precipitation occurs. H1 also showed a slightly higher runoff compared to H2 and H3, most likely due to the very sudden peak in the beginning of the cloudburst.

It is important to note that in figures 15 and 16 the maximum runoff given by the the highest compaction degree reflects a situation where very heavy machinery is used (grain harvesting and cotton harvesting equipment). Situations where similar force are applied in an urban environment are rare and would only occur during landscaping projects or when construction machines are passing over the area. These scenarios therefor have a possibility to correlate with the maximum runoff coefficient in the above mentioned figures. Scenarios where the urban environment is exposed to cattle, foot traffic or sport events most likely correlate to a surface runoff showed for scenarios A0 - A1 and D0 - D1. As seen in the penetrologger measurements, light foot traffic can have a significant increase in resistance throughout the soil profile, so there is a possibility that

with time, even light force application - such as foot traffic - can cause runoff similar to scenarios A2 and D3. Other factors apart from the loading weight is also relevant. Wet conditions would render the soil more sensitive to compaction and could result in compaction scenarios closer to to right side on the X-axis in figure 15 and 16, even if the applied force is relatively small.

5.3 Future studies

During the researching stage of this paper, it is noted that not much information or previous research has been conducted regarding FTCs and compaction. Although part of the original ambition for this report, it was not possible to conduct field experiments on the soil relating to FTCs due to the time span of this report. Ideally, samples would need to be taken before and after the winter months when the soil goes through FTCs and compare for example bulk density, pore structure or alike. There is much to explore on the topic and it is highly relevant to the climate of Sweden as the soil goes through multiple FTCs.

There is also much of information available in the out-files from the simulations apart from the runoff values. Amongst them is the moisture content throughout the soil profile for each compaction level and soil. (Pitt et al. 2008) found that the antecedent soil moisture in sandy soils had little significance on the infiltration compared to compaction, whilst for clayey soils these two factors had similar significance. Therefore there is much more to explore in relation to compaction and moisture content.

There are many ways to expand on the topic with further studies. In this project, the soil texture is assumed to be homogenous in both the upper and lower layer, but having different layers would be more realistic as variation is not uncommon. The simulated values in this report can also be used as input-data in other models focused on 2D/3D overland runoff flow and how this affects different communities and cities.

5.4 Future management

Compaction is generally a highly explored topic within the agricultural industry, as it has a significant affect on the harvest each year and many studies used in this report are focused on soil dynamics specified for the agricultural sector. One of the ways to remedy the compaction from harvesting equipment and alike is to tillage the soil (Hu et al. 2018). No such opportunity exists for urban green areas as that would disrupt the vegetation cover and remove it's ecosystem services catering to recreational activities and visual aesthetic. Even within agriculture, tilling the subsoil is a difficult task. This highlights the significance of how urban green areas are managed, and how we estimate runoff and storm water management. The general take away from this project would be use more sand-rich soils for parks to help mitigate the risk of runoff. Since both the sandy loam and loamy sand are two soils recommended for landscaping, one would rather opt for the loamy sand as this one contains a higher fraction of sand. Another recommendation would be to avoid heavy vehicles passing on the urban green areas if possible, as this has shown to decrease the infiltration significantly.

As mentioned in the theory, wet soil is more vulnerable to compaction, Therefore heavy machinery should be avoided during landscaping projects and construction to reduce the effect of compaction, especially during wet soil conditions. As mentioned by Burghardt & Schneider (2018) a higher organic matter content can also help decrease the effects of compaction, Therefore addition of this could be an option when designing urban landscapes. There are also ways to increase the soils infiltration. Bartens et al. (2008) found that the presence of certain tree types can increase infiltration in the soil due to the developed root system.

It is overall essential to consider and clarify during urban planning projects how much the green areas are supposed to infiltrate during heavy rainfall and how much is supposed to be managed by existing storm water management systems, to better utilize both systems. The next step is to foster the soils infiltration capacity through the help of some of the methods mentioned above such as using more sandy soils, avoiding heavy vehicle traffic etc.

6 Conclusion

By gathering information from studies based on agricultural conditions and applying them to this project, the knowledge regarding how soil compaction affects urban environments has been expanded and tested through both modelling and field experiments. The most important results found in this study is that that the runoff coefficient increases with increasing soil compaction, but that that the most crucial factor for runoff is soil texture. The field experiments showed clearly that the infiltration decreased with increasing number of vehicle passes. But bulk density did not show an increase with increase number of vehicle passes, most likely due to the heterogeneity of the soil or the vehicle used was relatively light to have an affect on bulk density at the sample depth. A summary of the answers to the problem statements is presented as bullet points below.

- **What are some sources to soil compaction in urban environments?** The main cause of compaction is applied force, and in urban environments this would be due to the use of vehicles for construction work or alike. The field experiments also showed a higher penetration resistance for the measurements taken in a pathway for two of the sites. This indicates that foot-traffic, although very light in comparison to other causes, is also a cause of compaction in urban green areas over time, in a similar way that cattle has been found to compact soils on pastures.
- **How does the freeze/thaw process affect the soil properties?** For coarser grained soils like sand, FTCs increase particle fragmentation. For fine-grained soils FTCs increase aggregate stabilization. FTC can also partially restore soils to conditions prior to compaction, but have minimal effect below a depth of 40 cm.
- **How does the infiltration rate vary with soil compaction?** From the field experiments, it is seen that increased number of vehicle passes decreases the infiltration rate for all three sites tested. The modelling simulations also show more runoff with increasing compaction, wich points to a decrease in infiltration in the soil.
- **How does the soil properties vary with soil compaction?** The field experiments showed no correlation between bulk density and compaction, despite the presumption that it would. This is attributed to the heterogeneity of the soil as well as a too light of a vehicle being used for the experiments. The infiltration rate decreased with increased number of vehicle passes. The soil penetration resistance increased with number of vehicle passes for one of the sites and showed a significant difference between the untouched soil compared to the measurements taken in the pathway. The remaining site showed no clear correlation, which was attributed to difficult weather conditions and unknown underlying materials.
- **How does the soil compaction affect the surface runoff in urban environments?** Based on the soil simulations done in HYDRUS-1D there is a clear correlation between amount of runoff and soil compaction as the runoff coefficient increases with increasing compaction for all soils simulated. The runoff coefficient also increases with the return period of the rain events when observing the simulations based on soils found in urban environments.
- **What significance does soil compaction have on surface runoff rate compared to other parameters?** A higher sand content mitigates the effects of soil compaction and leads

to less runoff. When comparing a sandy loam and a clay soil it is concluded that the sandy loam is more sensitive to soil compaction as more compaction leads to more runoff compared to the non-compacted scenario. The clay soil has little variation between the compaction scenarios but has generally more surface runoff in total. Soil texture Therefore affects the surface runoff more than soil compaction.

References

Agronomic Crops Network (n.d.).
URL: *https://agcrops.osu.edu/newsletter/corn-newsletter/2018-03/soil-infiltration*

Bartens, J., Day, S. D., Harris, J. R., Dove, J. E. & Wynn, T. M. (2008), 'Can urban tree roots improve infiltration through compacted subsoils for stormwater management?', *Journal of Environmental Quality* **37**, 2048–2057.

Batey, T. (2009), 'Soil compaction and soil management – a review', *Soil Use and Management* **25**, 335–345.

Batey, T. & McKenzie, D. C. (2006), 'Soil compaction: identification directly in the field', *Soil Use and Management* **22**, 123–131.

Broekhuizen, I., Sandoval, S., Gao, H., Mendez-Rios, F., Leonhardt, G., Bertrand-Krajewski, J. L. & Viklander, M. (2021), 'Performance comparison of green roof hydrological models for full-scale field sites', *Journal of Hydrology X* **12**, 100093.

Burghardt, W. & Schneider, T. (2018), 'Bulk density and content, density and stock of carbon, nitrogen and heavy metals in vegetable patches and lawns of allotments gardens in the northwestern ruhr area, germany', *Journal of Soils and Sediments* **18**, 407–417.

Chamberlain, E. J. & Gow, A. J. (1979), 'Effect of freezing and thawing on the permeability and structure of soils', *Engineering Geology* **13**, 73–92.

Chow, V. T., Maidment, D. R. & Mays, L. W. (1988), *Applied Hydrology*.

da Silveira, A. L. L. (2016), 'Cumulative equations for continuous time chicago hyetograph method'.

D'Acqui, L. P., Certini, G., Cambi, M. & Marchi, E. (2020), 'Machinery's impact on forest soil porosity', *Journal of Terramechanics* **91**, 65–71.

Daniel, J. A., Potter, K., Altom, W., Aljoe, H. & Stevens, R. (2002), 'Long–term grazing density impacts on soil compaction', *Transactions of the ASAE* **45**, 1911–.

Davies, D. B., Finney, J. B. & Richardson, S. J. (1973), 'Relative effects of tractor weight and wheel-slip in causing soil compaction'.

Deb, S. K. & Shukla, M. K. (2012), 'Variability of hydraulic conductivity due to multiple factors', *American Journal of Environmental Sciences* **8**, 489–502.

Dourado Neto, D., de Jong van Lier, Q., van Genuchten, M., Reichardt, K., Metselaar, K. & Nielsen, D. (2011), 'Alternative analytical expressions for the general van genuchten–mualem and van genuchten–burdine hydraulic conductivity models', *Vadose Zone Journal* **10**(2), 618–623.

Duan, R., Fedler, C. B. & Borrelli, J. (2011), 'Field evaluation of infiltration models in lawn soils', *Irrigation Science* **29**, 379–389.

Duiker, S. W. (2005), 'Avoiding soil compaction'.
URL: *https://extension.psu.edu/avoiding-soil-compaction*

Ekwue, E. I. & Stone, R. J. (1995), 'Organic matter effects on the strength properties of compacted agricultural soils', *Transactions of the ASAE* **38**, 357–365.

Eriksson, J., Dahlin, S., Nilsson, I. & Simonsson, M. (2019), *Marklära*, Studentlitteratur.

Folorunso, O. A., Rolston, D. E., Prichard, T. & Loui, D. T. (1992), 'Soil surface strength and infiltration rate as affected by winter cover crops', *Soil Technology* **5**, 189–197.

Fouli, Y., Cade-Menun, B. J. & Cutforth, H. W. (2013), 'Freeze-thaw cycles and soil water content effects on infiltration rate of three saskatchewan soils', *Canadian Journal of Soil Science* **93**, 485–496.

Fryksten, J. & Nilfouroushan, F. (2019), 'Analysis of clay-induced land subsidence in uppsala city using sentinel-1 sar data and precise leveling', *Remote Sensing 2019, Vol. 11, Page 2764* **11**, 2764.

Goutal, N., Boivin, P. & Ranger, J. (2012), 'Assessment of the natural recovery rate of soil specific volume following forest soil compaction', *Soil Science Society of America Journal* **76**, 1426–1435.

Gregory, J., Dukes, M., Jones, P. & Miller, G. (2006), 'Effect of urban soil compaction on infiltration rate', *Journal of Soil and Water Conservation* **61**, 117–124.

Hamilton, G. & Waddington, D. (1999), 'Infiltration rates on residential lawns in central pennsylvania', *Journal of Soil and Water Conservation* **54**, 564–568.

Hilten, R. N., Lawrence, T. M. & Tollner, E. W. (2008), 'Modeling stormwater runoff from green roofs with hydrus-1d', *Journal of Hydrology* **358**, 288–293.

Hu, W., Tabley, F., Beare, M., Tregurtha, C., Gillespie, R., Qiu, W. & Gosden, P. (2018), 'Short-term dynamics of soil physical properties as affected by compaction and tillage in a silt loam soil', *Vadose Zone Journal* **17**, 1–13.

Hydrus-1D Forum (n.d.).
URL: *https://www.pc-progress.com/forum/viewtopic.php?f=1t=137*

Håkansson, I. & Petelkau, H. (1994), 'Benefits of limited axle load', *Developments in Agricultural Engineering* **11**, 479–499.

IDF SMHI (n.d.).
URL: *https://www.smhi.se/klimat/framtidens-klimat/skyfallsstatistik-regional-statistik-for-extrema-korttidsregn*

Jabro, J. D., Iversen, W. M., Evans, R. G., Allen, B. L. & Stevens, W. B. (2014), 'Repeated freeze-thaw cycle effects on soil compaction in a clay loam in northeastern montana', *Soil Science Society of America Journal* **78**, 737–744.

Lan, T., Guo, S. W., Han, J. W., Yang, Y. L., Zhang, K., Zhang, Q., Yang, W. & Li, P. F. (2019), 'Evaluation of physical properties of typical urban green space soils in binhai area, tianjin, china', *Urban Forestry Urban Greening* **44**, 126430.

Lehrsch, G. A. (1998), 'Freeze-thaw cycles increase near-surface aggregate stability', *Soil Science* **163**, 63–70.

Molina, A., Govers, G., Vanacker, V., Poesen, J., Zeelmaekers, E. & Cisneros, F. (2007), 'Runoff generation in a degraded andean ecosystem: Interaction of vegetation cover and land use', *CATENA* **71**, 357–370.

MSB (2013), 'Pluviala översvämningar : konsekvenser vid skyfall över tätorter, en kunskapsöversikt'.

Mulholland, B. & Fullen, M. A. (1991), 'Cattle trampling and soil compaction on loamy sands', *Soil Use and Management* **7**, 189–193.

Ngo-Cong, D., Antille, D. L., van Genuchten, M. T., Nguyen, H. Q., Tekeste, M. Z., Baillie, C. P. & Godwin, R. J. (2021), 'A modeling framework to quantify the effects of compaction on soil water retention and infiltration', *Soil Science Society of America Journal* **85**, 1931–1945.

Nilsson, E. (2023), 'Surface runoff on green urban areas : A study on driving forces behind surface runoff generaiton'.

Ohu, J. O., Raghavan, G. S. & McKyes, E. (1985), 'Peatmoss effect on the physical and hydraulic characteristics of compacted soils.', *Transactions of the American Society of Agricultural Engineers* **28**, 420–424.

Olson, N. C., Gulliver, J. S., Nieber, J. L. & Kayhanian, M. (2013), 'Remediation to improve infiltration into compact soils', *Journal of Environmental Management* **117**, 85–95.

Olsson, J., Berg, P., Eronn, A., Simonsson, L., Södling, J., Wern, L. & Yang, W. (2017), 'Extremregn i nuvarande och framtida klimat analyser av observationer och framtidsscenarier', *KLIMATOLOGI Nr* **47**.

Osunbitan, J. A., Oyedele, D. J. & Adekalu, K. O. (2005), 'Tillage effects on bulk density, hydraulic conductivity and strength of a loamy sand soil in southwestern nigeria', *Soil and Tillage Research* **82**, 57–64.

Pitt, R., Chen, S. E. & Clark, S. (2002), 'Compacted urban soils effects on infiltration and bioretention stormwater control designs', *Global Solutions for Urban Drainage* pp. 1–21.

Pitt, R., Chen, S.-E., Clark, S. E., Swenson, J. & Ong, C. K. (2008), 'Compaction's impacts on urban storm-water infiltration', *Journal of Irrigation and Drainage Engineering* **134**, 652–658.

Pulido-Moncada, M., Munkholm, L. J. & Schjønning, P. (2019), 'Wheel load, repeated wheeling, and traction effects on subsoil compaction in northern europe', *Soil and Tillage Research* **186**, 300–309.

Rai, R. K., Singh, V. P. & Upadhyay, A. (2017), 'Soil analysis', *Planning and Evaluation of Irrigation Projects* pp. 505–523.

Reynolds, W. D., Galloway, K. & Radcliffe, D. E. (n.d.), 'The relationship between perc time and field-saturated hydraulic conductivity for cylindrical test holes'.

Schaap, M. G., Leij, F. J. & Genuchten, M. T. V. (2001), 'Rosetta: A computer program for estimating soil hydraulic parameters with hierarchical pedotransfer functions', *Journal of Hydrology* **251**, 163–176.

Sharifi, A., Godwin, R. J., O'Dogherty, M. J. & Dresser, M. L. (2007), 'Evaluating the performance of a soil compaction sensor', *Soil Use and Management* **23**, 171–177.

Simonovic, S. P. & Nirupama, N. (2007), 'Increase of flood risk due to urbanisation: A canadian example system dynamics simulation for assessment of hydropower dam safety view project comett project view project increase of flood risk due to urbanisation: A canadian example'.

Singh, J. & Kaul, A. (2015), 'Impact of soil compaction on soil physical properties and root growth: A review agronomic evaluation and field demonstration of millets cultivation to enhance livelihood security and crop diversification in punjab view project project work view project'.

Sinnett, D., Poole, J. & Hutchings, T. R. (2006), 'The efficacy of three techniques to alleviate soil compaction at a restored sand and gravel quarry', *Soil Use and Management* **22**, 362–371.

Soane, B. D. (1990), 'The role of organic matter in soil compactibility: A review of some practical aspects', *Soil and Tillage Research* **16**, 179–201.

Statista (n.d.), 'Number of deaths due to floods worldwide from 1960 to 2020'.
URL: *https://www.statista.com/statistics/1293207/global-number-of-deaths-due-to-flood/*

Svenskt Vatten (2011), 'Nederbördsdata vid dimensionering och analys av avloppssystem'.

Swedish University of Agricultural Sciences (n.d.), 'Lantmät'.
URL: *https://www.slu.se/fakulteter/nj/om-fakulteten/centrumbildningar-och-storre-forskningsplattformar/faltforsk/vader/lantmet/*

Thompson, A. L. & James, L. G. (1985), 'Water droplet impact and its effect on infiltration', *Transactions of the ASAE* **28**, 1506–1510.

Tian, Z., Gao, W., Kool, D., Ren, T., Horton, R. & Heitman, J. L. (2018), 'Approaches for estimating soil water retention curves at various bulk densities with the extended van genuchten model', *Water Resources Research* **54**, 5584–5601.

Unger, P. W. & Kaspar, T. C. (1994), 'Soil compaction and root growth: A review', *Agronomy Journal* **86**, 759–766.

United States Department of Agriculture (n.d.*a*), 'Rosetta model'.
URL: *https://www.ars.usda.gov/pacific-west-area/riverside-ca/agricultural-water-efficiency-and-salinity-research-unit/docs/model/rosetta-model/*

United States Department of Agriculture (n.d.*b*), 'Soil infiltration'.
URL: *https://web.archive.org/web/20200208195848/ https://www.nrcs.usda.gov/Internet/FSE*$_{D}OCUMENTS/nrcs142p2_{0}53268.pdf$

Viklander, P. (1997), 'Compaction and thaw deformation of frozen soil : permeability and structural effects due to freezing and thawing.'.

Voorhees, W. B., Senst, C. G. & Nelson, W. W. (1978), 'Compaction and soil structure modification by wheel traffic in the northern corn belt', *Soil Science Society of America Journal* **42**, 344–349.

Wang, Y., Gao, L., Huang, S. & Peng, X. (2022), 'Combined effects of rainfall types and antecedent soil moisture on runoff generation at a hillslope of red soil region', *European Journal of Soil Science* **73**.

Weil, R. R. & Brady, N. C. (1999), *The Nature and properties of soils*, 12 edn, Prentice Hall.

Yang, J. L. & Zhang, G. L. (2011), 'Water infiltration in urban soils and its effects on the quantity and quality of runoff', *Journal of Soils and Sediments* **11**, 751–761.
URL: *https://link.springer.com/article/10.1007/s11368-011-0356-1*

Yasuda, H., Katsura, M. & Katsuragi, H. (2023), 'Grain-size dependence of water retention in a model aggregated soil', *Advanced Powder Technology* **34**, 103896.

Zhang, Z., Ma, W., Feng, W., Xiao, D. & Hou, X. (2016), 'Reconstruction of soil particle composition during freeze-thaw cycling: A review', *Pedosphere* **26**, 167–179.

7 Appendix

7.1 Appendix A: Lab measurements and calculations

		Cylinder	Cylinder + wet soil	Wet soil	Cylinder + dry soil	Dry soil	Moisture content (%)	Average weight (g)	Volume (cm)	Bulk density	Average bulk density	Average moisture
Ångströms	F0A	145,108	501,82	356,712	462,98	317,872	10,8883357	285,784	199,504	1,5933	1,432474687	14,25821179
	F0B	149,76	475,13	325,37	424,07	274,31	15,6929035			1,375	1,352055126	
	F0C	140,8	486,91	346,11	405,97	265,17	23,3856288			1,3291		
	F1A	143,41	475,05	331,64	438,46	295,05	11,0330479	276,8367		1,4789	1,38762673	
	F1B	132,52	438,02	305,5	406,18	273,66	10,4222586			1,3717		
	F1C	149,41	454,37	304,96	411,21	261,8	14,1526758			1,3123		
	F2A	153,28	457,3	304,02	405,41	252,13	17,0679561	255,05		1,2638	1,278422406	
	F2B	144,73	445,38	300,65	406,82	262,09	12,8255447			1,3137		
	F2C	147,14	448,6	301,46	398,07	250,93	16,7617594			1,2578		
	Fmax1	147,54	482,29	334,75	437,9	290,36	13,2606423	285,62		1,4554	1,431652647	
	Fmax2	145,61	462,45	316,84	426,49	280,88	11,3495771			1,4079		
										0		
Geocentrum	G0A	150,34	501,27	350,93	432,9	282,56	19,4825179	270,93		1,4163	1,358019927	19,92298465
	G0B	152,32	480,25	327,93	413,74	261,42	20,2817675			1,3104		
	G0C	150,68	481,27	330,59	419,49	268,81	18,6878006			1,3474		
	G1A	151,43	485,69	334,26	420,39	268,96	19,5356908	275,82		1,3481	1,382530751	
	G1B	150,98	500,17	349,19	435,54	284,56	18,5085484			1,4263		
	G1C	150,56	490,31	339,75	424,5	273,94	19,3701251			1,3731		
	G2A	150,37	485,62	335,25	423,24	272,87	18,6070097	244,4067		1,3677	1,225073354	
	G2B	151,85	424,45	272,6	360,22	208,37	23,5619956			1,0444		
	G2C	152,04	470,3	318,26	404,02	251,98	20,82574			1,263		
	Gmax1	151,66	497,75	346,09	428,02	276,36	20,1479384	276		1,3852	1,38343299	
	Gmax2	150,31	495,48	345,17	425,95	275,64	20,1436973			1,3816		
										0		
BMC	H0A	151,99	536,44	384,45	474,73	322,74	16,0515021	305,6833		1,6177	1,532218869	16,0849463
	H0B	152,35	475,85	323,5	426,46	274,11	15,2673879			1,374		
	H0C	142,13	515,19	373,06	462,33	320,2	14,1693025			1,605		
	H1A	147,91	499,08	351,17	440,33	292,42	16,729789	268,4567		1,4657	1,345622496	
	H1B	149,49	497,56	348,07	433,41	283,92	18,4302008			1,4231		
	H1C	150,32	422,4	272,08	379,35	229,03	15,8225522			1,148		
	H2A	135,41	521,85	386,44	456,02	320,61	17,034986	298,0933		1,607	1,494174462	
	H2B	150,89	484,4	333,51	426,32	275,43	17,4147702			1,3806		
	H2C	143,83	495,02	351,19	442,07	298,24	15,0773086			1,4949		
	Hmax1	144,55	514,13	369,58	459,03	314,48	14,9088154	303,465		1,5763	1,52109961	
	Hmax2	145,83	494,1	348,27	438,28	292,45	16,0277945			1,4659		

Figure 17: Calculations and measured values from laboratory. The purple marks indicating a comment in the cells is used to note which cylinder had the presence of a noticeably larger rock.

Soil texture							Procent		
		Lera (cm)	Silt (cm)	Sand (cm)	Total (cm)		**Lera**	**Silt**	**Sand**
Ångström	F	0,2	2,4	7,8	10,4		1,923077	23,07692	75
Geocentrum	G	0	3,4	11,2	14,6		0	23,28767	76,71233
EBC	H	0,2	2,8	12	15		1,333333	18,66667	80

Figure 18: Soil texture

		Crucible	*Crucible + dry soil*	*Dry soil*	*Crucible + burned*	*Burned soil*	*Organic matter content (%)*	*Average value*
Ångström	F0A	31,445	74,2399	42,795	73,1443	41,6993	2,560118145	4,24958
	F0B	29,07	56,8891	27,819	55,7887	26,7187	3,955555715	
	F0C	29,0208	56,484	27,463	54,7722	25,7514	6,233068251	
	F1A							
	F1B							
	F1C							
	F2A							
	F2B							
	F2C							
	Fmax1							
	Fmax2							
Geocentrum	G0A	33,9305	75,4972	41,567	73,167	39,2365	5,605929747	5,88839
	G0B	31,6239	69,5937	37,97	66,9885	35,3646	6,861242356	
	G0C	32,5559	72,1136	39,558	69,919	37,3631	5,547845299	
	G1A	31,8855	64,1444	32,259	62,2121	30,3266	5,98997486	
	G1B	29,9	53,9337	24,034	52,6633	22,7633	5,285911033	
	G1C	28,713	49,6682	20,955	48,4564	19,7434	5,782812858	
	G2A	29,7042	60,3317	30,628	58,8798	29,1756	4,740510979	
	G2B	29,232	50,9925	21,761	49,4133	20,1813	7,257186186	
	G2C	23,3842	53,2562	29,872	51,3184	27,9342	6,487011248	
	Gmax1	23,3002	46,5032	23,203	45,119	21,8188	5,965607896	
	Gmax2	25,7816	54,5017	28,72	52,9944	27,2128	5,248240779	
EBC	H0A	29,2855	51,9493	22,664	50,8397	21,5542	4,895913307	4,85615
	H0B	27,9622	52,8422	24,88	51,4222	23,46	5,707395498	
	H0C	29,2922	56,5958	27,304	55,0552	25,763	5,64247938	
	H1A	22,3747	47,9263	25,552	46,8683	24,4936	4,140640899	
	H1B	30,1476	50,2579	20,11	49,1332	18,9856	5,592656499	
	H1C	25,6807	49,6798	23,999	48,5448	22,8641	4,729344017	
	H2A	26,6162	56,7837	30,168	55,2809	28,6647	4,981519848	
	H2B	28,967	53,9027	24,936	52,1811	23,2141	6,904157493	
	H2C	30,7717	56,3778	25,606	55,5846	24,8129	3,097699376	
	Hmax1	28,4463	54,6459	26,2	53,6819	25,2356	3,679445488	
	Hmax2	23,4121	53,9013	30,489	52,6676	29,2555	4,046350839	

Figure 19: Organic matter content

7.2 Appendix B: T-test

Bulk density data t-test

[a]

	T-test	Geocentrum		
	0	2	10	Max
0		0,56065	0,2551	0,5713
2			0,1834	0,97775
10				0,28814
Max				

[b]

	T-test	BMC		
	0	2	10	Max
0		0,216403	0,7299	0,92602
2			0,2804	0,28445
10				0,79297
Max				

[c]

	T-test	Ångström		
	0	2	10	Max
0		0,661389	0,1385	0,99434
2			0,1031	0,54905
10				0,01314
Max				

Figure 20: Resulting p-values for the t-test conducted on the bulk density samples for the three sites where a) Geocentrum, b) BMC, c) Ångström.

[a]

	T-test	0 - 10 cm	Geocentrum	
	0	2	10	Max
0		0,123708345	0,41972747	0,006319914
2			0,478100662	0,061293116
10				0,024148072
Max				

[b]

	T-test	0 -10 cm	BMC	
	0	2	10	Max
0		1,28962E-05	1,7482E-05	5,8463E-09
2			0,110000063	0,000430151
10				0,300385283
Max				

[c]

	T-test	0-10 cm	Ångström	
	0	2	10	Max
0		0,369858	0,577232741	0,450849506
2			0,096913977	0,084342127
10				0,797415834
Max				

Figure 21: Resulting p-values for the t-test conducted on the penetrologger measurements for the depth 0 - 10 cm where a) Geocentrum, b) BMC, c) Ångström.

Penetrologger measurement t-test

[a]

	T-test	10 - 30 cm	Geocentrum	
	0	2	10	Max
0		3,08012E-07	0,001008796	5,11767E-10
2			0,003827023	0,579854234
10				0,000630044
Max				

[b]

	T-test	10 - 30 cm	BMC	
	0	2	10	Max
0		6,08336E-12	1,7556E-20	7,3537E-21
2			2,42097E-10	4,49796E-14
10				0,00043212
Max				

[c]

	T-test	10 - 30 cm	Ångström	
	0	2	10	Max
0		0,061905	1,8392E-05	5,30711E-15
2			0,000624745	1,55469E-12
10				0,004170939
Max				

Figure 22: Resulting p-values for the t-test conducted on the penetrologger measurements for the depth 10 - 30 cm where a) Geocentrum, b) BMC, c) Ångström.

[a]

	T-test	30 - 50 cm	Geocentrum	
	0	2	10	Max
0		2,4977E-18	0,589772606	2,10002E-21
2			7,15524E-25	7,15524E-25
10				1,4476E-19
Max				

[b]

	T-test	30 - 50 cm	BMC	
	0	2	10	Max
0		1,65941E-07	6,18683E-28	6,92276E-33
2			3,39368E-18	2,09376E-28
10				0,000114745
Max				

[c]

	T-test	30 - 50 cm	Ångström	
	0	2	10	Max
0		0,005639	5,51295E-40	3,08285E-47
2			3,99156E-19	1,29229E-23
10				7,06067E-32
Max				

Figure 23: Resulting p-values for the t-test conducted on the penetrologger measurements for the depth 30 - 50 cm where a) Geocentrum, b) BMC, c) Ångström.

7.3 Appendix C: Simulation summary runoff values

Summary of all the simulations

		2 year					10 year					100 year					2 year	10 year	100 year
		H1	H2	H3	H4	H5	H1	H2	H3	H4	H5	H1	H2	H3	H4	H5	CDS	CDS	CDS
A: Sandy loam	A0	0,190	0,092	0	0,313	0,267	0,333	0,230	0,220	0,426	0,363	0,485	0,437	0,443	0,538	0,517	0,318	0,415	0,555
	A1	0,277	0,185	0,185	0,397	0,349	0,401	0,340	0,351	0,489	0,454	0,563	0,527	0,557	0,620	0,612	0,395	0,493	0,631
	A2	0,385	0,313	0,215	0,477	0,436	0,496	0,454	0,482	0,567	0,557	0,658	0,650	0,660	0,696	0,696	0,487	0,585	0,711
	A3	0,523	0,482	0,472	0,590	0,574	0,638	0,621	0,633	0,674	0,674	0,772	0,774	0,772	0,781	0,781	0,605	0,691	0,808
B: Loamy sand	B0	0	0	0	0	0	0	0	0	0	0	0,072	0	0	0,127	0,044	0	0	0,118
	B1	0	0	0	0	0	0	0	0	0,005	0	0,118	0,004	0	0,181	0,089	0	0,011	0,175
	B2	0	0	0	0	0	0	0	0	0,082	0,020	0,196	0,049	0,004	0,249	0,169	0	0,074	0,243
	B3	0	0	0	0,056	0,005	0,099	0,005	0	0,191	0,103	0,302	0,137	0,068	0,331	0,259	0,051	0,177	0,333
C: Sand	C0	0	0	0	0	0	0	0	0	0	0	0	0	0	0	0	0	0	0
	C1	0	0	0	0	0	0	0	0	0	0	0	0	0	0	0	0	0	0
	C2	0	0	0	0	0	0	0	0	0	0	0	0	0	0	0	0	0	0
	C3	0	0	0	0	0	0	0	0	0	0	0	0	0	0	0	0	0	0
D: Clay	D0	0,549			0,615	0,605	0,667		0,674		0,706	0,793	0,797	0,795	0,802	0,812	0,610	0,713	0,823
	D1	0,605		0,610	0,656	0,651	0,709		0,716		0,745	0,827	0,829	0,829	0,829	0,838	0,656	0,755	0,852
	D2			0,667	0,697	0,703	0,759		0,766		0,780	0,859	0,861	0,859	0,861	0,865	0,708	0,791	0,873
	D3																0,759	0,830	0,901
E: Silt loam	E0	0,123	0,087	0	0,164	0,082	0,259	0,064	0,007	0,277	0,184	0,418	0,215	0,137	0,378	0,329	0,185	0,273	0,384
	E1	0,144	0,111	0	0,195	0,097	0,277	0,078	0,013	0,284	0,195	0,219	0,232	0,158	0,388	0,346	0,195	0,284	0,397
	E2																		
	E3	0,236	0,236	0,008	0,267	0,185	0,355	0,163	0,082	0,348	0,284	0,487	0,348	0,289	0,451	0,420	0,267	0,351	0,462

Surface runoff (cm)										
0 - 0,1	0,1 - 0,2	0,2 - 0,3	0,3 - 0,4	0,4 - 0,5	0,5 - 0,6	0,6 - 0,7	0,7 - 0,8	0,8 - 0,9	0,9 - 1	Crash

Figure 24: Runoff coefficient for each type of soil, degree of compaction, hyetograph and 2,10 and 100-year rain